Surprising concentrations of hydrogen and non-geological methane and carbon dioxide in the soil

Etiope G.[1,2*], Ciotoli G.[3,1], Benà E.[4], Mazzoli, C.[4], Röckmann T.[5], Sivan M.[5], Squartini A.[6], Laemmel T.[7], Szidat S.[7], Haghipour N.[8], Sassi R.[4]

[1] *Istituto Nazionale di Geofisica e Vulcanologia, Sezione Roma2, Rome, Italy*
[2] *Faculty of Environmental Science and Engineering, Babes-Bolyai University, Cluj-Napoca, Romania*
[3] *Consiglio Nazionale delle Ricerche, Istituto di Geologia Ambientale e Geoingegneria, Monterotondo, Italy*
[4] *Dipartimento di Geoscienze, Università di Padova, Padova, Italy*
[5] *Institute for Marine and Atmospheric Research Utrecht, Utrecht University, The Netherlands*
[6] *Department of Agronomy, Food, Natural Res., Animals and Environment, Università di Padova, Padova, Italy*
[7] *Department of Chemistry, Biochemistry and Pharmaceutical Sciences & Oeschger Center for Climate Change Research, University of Bern, Bern, Switzerland*
[8] *Geological Institute & Laboratory of Ion Beam Physics, ETHZ, Zurich, Switzerland*
**Corresponding author: giuseppe.etiope@ingv.it*

Abstract

Due to its potential use as a carbon-free energy resource with minimal environmental and climate impacts, natural hydrogen (H_2) produced by subsurface geochemical processes is today the target of intensive research. In H_2 exploration practices, bacteria are thought to swiftly consume H_2 and, therefore, small near-surface concentrations of H_2, even orders of 10^2 ppmv in soils, are considered a signal of active migration of geological gas, potentially revealing underground resources. Here, we document an extraordinary case of a widespread occurrence of H_2 (up to 1 vol.%), together with elevated concentrations of CH_4 and CO_2 (up to 51 and 27 vol.%, respectively), in aerated meadow soils along Italian Alps valleys. Based on current literature, this finding would be classified as a discovery of pervasive and massive geological H_2 seepage. Nevertheless, an ensemble of gas geochemical and soil microbiological analyses, including bulk and clumped CH_4 isotopes, radiocarbon of CH_4 and CO_2, and DNA and *mcrA* gene quantitative polymerase chain reaction analyses, revealed that H_2 was only coupled to modern microbial gas. The H_2-CO_2-CH_4-H_2S association, wet soil proximity, and the absence of other geogenic gases in soils and springs suggest that H_2 derives from near-surface fermentation, rather than geological degassing. H_2 concentrations

up to 1 vol.% in soils are not conclusive evidence of deep gas seepage. This study provides a new reference for the potential of microbial H_2, CH_4 and CO_2 in soils, to be considered in H_2 exploration guidelines and soil carbon and greenhouse-gas cycle research.

Keywords: Natural hydrogen, methane, carbon dioxide, soil-gas, radiocarbon

1. Introduction

Natural hydrogen gas (H_2) produced by a variety of geochemical processes in crustal and mantle rocks is currently sought-after for its use as a carbon-free energy resource with low environmental and climate impacts (e.g., Gaucher, 2020; Rigollet and Prinzhofer, 2022; Yedinak, 2022). Together with artificially produced hydrogen (e.g., black/gray, blue, green hydrogen; IEA, 2023) and the hydrogen generation stimulated by geochemical reactions in the underground (orange hydrogen; Osselin et al. 2022), the naturally occurring geological H_2 (also referred to as "white" or "gold" hydrogen) might contribute to new hydrogen economy implementation. The geochemical processes generating subsurface H_2 are mostly related to water-rock reactions such as serpentinization (olivine hydration), radiolysis, and several types of iron oxidation (Sherwood Lollar et al. 2014; Warr et al. 2019; Zgonnik, 2020; Milkov, 2022; Geymond et al. 2023). Relevant amounts (up to 98 vol.%) of H_2 have been directly discovered in reservoirs intercepted by wells in the United States, Mali, Australia, and the Russian Federation (Newell et al 2007; Prinzhofer et al. 2018; Boreham et al. 2021; Zgonnik, 2020 and references therein). In other countries, H_2 is increasingly reported at the surface in soil or gas seeps (Zgonnik, 2020; Vacquand et al. 2018; Etiope, 2023; McMahon et al. 2023), and surface geochemistry is becoming part of global H_2 exploration (Lefeuvre et al. 2021; Frery et al. 2021; Lévy et al. 2023; Langhi and Strand, 2023). In soil-gas prospections, diffuse application of a paradigm exists by which H_2 microbially generated in wet soils and aquifers is rapidly consumed by bacteria and it should not occur in the aerated vadose zone (e.g., Rhee et al. 2006; Larin et al. 2015; Zgonnik

et al. 2015; Paulot et al. 2021). Therefore, the presence of H_2 in soil-gas, at concentrations on the order of 10^1-10^3 parts per million by volume (ppmv), is thought to be evidence of non-exogenous sources, i.e., geological degassing (seepage) from underground sources. This concept has been applied, for example, to so called "fairy circles" observed in Russia, the United States, Brazil, Australia, Namibia and Colombia (Larin et al. 2015; Zgonnik et al. 2015; Prinzhofer et al. 2019; Frery et al. 2021; Moretti et al., 2022; Carrillo Ramirez et al. 2023), to Pyrenean soils (Lefeuvre et al. 2021), to the San Andreas Fault in California (Mathur et al. 2023), and in proposed H_2 exploration guidelines (Lévy et al. 2023). However, similar amounts of H_2 can be produced by multiple microbially mediated processes, including fermentation in wet soils or shallow aquifers, N_2 fixation, and cellulose decomposition by termites (Conrad and Seilert, 1980; Krämer and Conrad, 1993; Sugimoto and Fujita, 2006; Pal et al. 2018), by the oxidation or corrosion of ferrous minerals (e.g., Starkey and Wight, 1945), and by the hydration of silicate radicals in basaltic soils (Dunham et al. 2021). Therefore, caution has been advised when cursorily attributing the term "seep" or "seepage" to soil-gas H_2 at ppmv levels (Etiope, 2023). H_2 may persist in soils due to inhibitors of syntrophic H_2 consumption such as hydrogen sulphide, alcohols, and organic acids (Hoeler et al. 1998; Schmidt et al. 2016; Meinel et al. 2022). The primary issue for understanding the H_2 potential in the soils is the paucity of available soil gas datasets. A few studies have focused on H_2 in soils as a tracer of faults and seismicity (e.g., Sugisaki et al., 1983; Xiang et al. 2020). Bio-ecosystem studies have largely addressed wetlands and the capacity of dry soil to act as an atmospheric H_2 sink, with a focus on laboratory tests and modelling, and without extensive *in situ* soil-gas surveys (e.g., Conrad 1996; Chen et al. 2015). As a result, insufficient data exists regarding background H_2 values, irrespective of soil moisture content or geological setting. Understanding the origin of H_2 in soil-gas is also complicated by the fact that biological and geological processes can produce H_2 with a similar isotopic composition ($^2H/H$, expressed as δ^2H), therefore, isotopic analyses may not be conclusive (Etiope, 2023). Given the issues outlined above, interpretations of H_2 origin should be based on a multidisciplinary, integrated study, including a compositional and isotopic analysis of the gases

86 associated with H_2. Careful investigations of the geology and the ecosystem are also necessary.
87 Here, we present an apparently straightforward case of relevant H_2 concentrations in aerated soils,
88 reaching 1 vol.%, which, based on current scientific literature, would immediately be classified as
89 the discovery of pervasive and massive geological H_2 seepage. The study was performed in two
90 valleys within the Eastern Alps (the Pusteria and Anterselva Valleys) of northern Italy, where high
91 H_2 values, associated with high methane (CH_4) values, were accidentally discovered in a previous
92 soil-gas survey addressed to radon. The H_2 and CH_4 data, not published in the radon study (Benà et
93 al. 2022), boosted the present study due to their noteworthy concentrations. Since elevated levels of
94 H_2 in aerated soils are commonly attributed to crustal degassing of geological origin (Larin et al.
95 2015; Zgonnik et al. 2015; Prinzhofer et al. 2019; Frery et al. 2021; Lefeuvre et al. 2021; Moretti et
96 al., 2022), our objective was to assess whether the high H_2 concentrations in the two Alpine valleys
97 are actually of geological origin or, rather, are a product of near-surface biological processes. To this
98 aim, we carried out an ensemble of gas geochemical and microbiological investigations (listed in
99 Table S1), including a wide soil-gas survey and multiple isotopic and radiocarbon analysis of CH_4
100 and CO_2 associated to H_2 in the soil. H_2 was also searched in several springs along the valleys. Surface
101 exploration of natural hydrogen has never made use of such an ensemble of analyses, particularly
102 radiocarbon analysis of CH_4 and CO_2 associated to H_2. Since the research was conceived as a surface
103 exploration of natural H_2 with the aim of understanding whether crustal degassing exists in the studied
104 area, investigating the specific biological and environmental elements that may have contributed to
105 the high levels of H_2 was beyond the scope of work. This study demonstrates the complexity of soil-
106 gas interpretations of H_2 and presents a crucial case to consider for future research and natural H_2
107 exploration guidelines.
108
109
110 **2. Geological setting of Pusteria and Anterselva valleys**
111

112 The Pusteria Valley develops along a segment of the Periadriatic lineament, the Pusteria Fault (PF),
113 which is an East–West trending, a sub vertical aseismic fault with dextral transpressive strike-slip
114 kinematics, representing the tectonic boundary between the Austroalpine crystalline basement to the
115 north and the Southalpine basement to the south (Fig. 1; Schmid et al. 1989).
116
117 *Figure 1*
118
119 The Austroalpine crystalline basement in the Eastern Alps consists of pre-Variscan sequences. These
120 were mainly affected by a Variscan (320-350 Ma) metamorphic event covering the whole temperature
121 range of the amphibolite and greenschist facies at metamorphic thermal gradients of about 40°C/km,
122 partly affected by Alpine metamorphic overprint (Sassi et al., 2004; Spiess et al., 2010). It is mainly
123 made up by paragneisses and micaschists (locally grading to migmatites), in which orthogneisses,
124 amphibolites, quartzites and marbles are interlayered. Eclogites, metabasites and metaultramafics
125 locally occur. The Southalpine crystalline basement in the Eastern Alps consists of a thick phyllitic
126 sequence affected by Variscan metamorphism under greenschist facies (Spiess et al. 2010). The
127 Austroalpine block is cut by two major E-W trending tectonic lines: the DAV (Defferegggen-
128 Antholz/Anterselva-Vals/Valles fault (DAV) and the KV (Kalkstein-Vallarga) faults (Fig. 1). The
129 DAV is a ~80 km long mainly mylonitic shear zone with dominant sinistral strike slip delimiting
130 towards the south the Alpine metamorphic overprint (Müller et al. 2000). The KV is a transpressive
131 strike-slip fault (Borsi et al., 1978). These two faults merge westwards close to the Insubric Line.
132 Based on seismic reflectors, Lammerer et al. (2011) suggest the presence of schists containing
133 serpentinites at depths of at least 5 km, in correspondence with the DAV and PF lineaments. The
134 Anterselva Valley, is NNE-SSW oriented, was formed by glacial excavation along both the
135 Austroalpine and Southalpine domains, and is crossed by the KV fault (Fig. 1). The soil features are
136 described in the Supplementary Material.
137

3. Methods

3.1 Sampling and the on-site analysis of gas in soils.

Soil-gas surveys were conducted during July 2021 (244 sampling points) and September 2021 (89 points, using two different sensors for both H_2 and CH_4, described below, with multiple measurements surrounding the H_2-rich points observed in July 2021). A check of H_2 and CH_4 was repeated in August 2023 (16 points; Fig. 1 and Tables S1 and S2). In addition to the Pusteria Valley, soil-gas surveys included the adjacent N-S trending Anterselva Valley, transversally crossed by a fault (Fig. 1). Soil-gas sampling, conducted during July and September 2021, and August 2023 (Tables S1 and S2), was performed by pounding stainless-steel probes with a sliding hammer to depths of 60-80 cm. To minimize soil moisture, soil and air temperature and barometric pressure effects (Hinkle, 1994), sampling was performed over a very short period of time and during stable meteorological conditions. The probe was then connected to the following portable gas detectors, for measuring H_2, CH_4, CO_2, O_2, and H_2S:

H_2: (a) A Dräger electrochemical sensor (DrägerSensor® XXS H_2, Dräger X-am 7000, Germany; accuracy ≤1% of measured value; range 0-2000 ppmv) used during July and September 2021, and August 2023; (b) A Huberg semiconductor + pellistor sensor (Huberg Metrex 2, Italy; range 0-5 vol.%; accuracy ≤2% at 1000 ppmv, and ≤1% at 10,000 ppmv) used during September 2021. Further details and sensor intercomparison tests are reported in the Supplementary Material.

CH_4: (a) A Dräger infrared sensor (DrägerSensor® Smart IR CH_4, Dräger X-am 7000, Germany; accuracy: ≤5%; range 0.1-100 vol.%) used during July and September 2021, and August 2023; (b) A Tunable Diode Laser Adsorption Spectrometry (TDLAS) detector (Gazomat, France; precision 0.1 ppmv, lower detection limit 0.1 ppmv; range 0-100 vol.%) used during September 2021.

CO_2: (a) A Dräger infrared sensor (DrägerSensor® Smart IR CO_2 HC, Dräger X-am 7000, Germany; accuracy: ≤0.2%; range 0-100 vol.%) used during July and September 2021, and August 2023; (b) A Licor non-dispersive infrared sensor (Licor LI-820; accuracy <3% of reading; range 0-20,000 ppmv)

used during September 2021.

O_2: (a) A Dräger electrochemical sensor (DrägerSensor® XXS O_2, Dräger X-am 7000, Germany; accuracy: ≤0.2%; range 0-25 vol.%) used during July and September 2021, and August 2023.

H_2S: (a) A Dräger electrochemical sensor (DrägerSensor® XXS H_2S, Dräger X-am 7000, Germany; precision: 0.5 ppmv; range 0-200 ppmv) used during July and September 2021, and August 2023.

The spatial distribution of H_2 and CO_2 in soil-gas along the Pusteria Valley was derived by Natural Neighbour interpolation of July 2021 soil-gas sampling points, using Surfer 23.1.162 (copyright 1993–2021, Golden Software, LLC).

H_2 and CH_4 fluxes from soils were measured using a closed chamber technique in 5 points at the P1 (Pusteria Valley) and A14 (Anterselva Valley) sites (Figure S1). A 30cm-diameter static accumulation chamber was connected to the semiconductor H_2 and laser CH_4 sensors described above, using the same procedure in Etiope (2023) and Etiope et al (2017).

At sites P1, P8, A14, and A15, soil-gas samples were collected for the laboratory analyses described below. Gas was stored in evacuated Teflon bags and Wheaton bottles sealed with gas impermeable, thick, blue butyl septa (Bellco Glass Inc., NJ, USA) and aluminum crimp caps.

3.2 Sampling and the on-site analysis of gas dissolved in spring water.

CH_4 and H_2 were analysed in five spring water samples collected along the Pusteria and Anterselva Valleys (the spring name and location are reported in Fig. 1). Dissolved gas was extracted via an equilibration head-space method in 500 mL Duran bottles, and analysed using the TDLAS (for CH_4) and the semiconductor sensor (for H_2) described above.

3.3 Laboratory analyses of gas samples.

3.3.1 Analysis of C_2-C_6 hydrocarbons.

189 The presence of C_{2+} volatile hydrocarbons (ethane, propane, butane, pentane, and hexane) in the four,
190 high-CH_4 soil-gas samples, stored in Teflon bags, was checked by Fourier Transform Infrared
191 Spectroscopy (FTIR, Gasmet DX-4030, Finland; lower detection limit 1 ppmv, accuracy ±10%).
192
193 *3.3.2 CH_4 and CO_2 isotopic analyses.*
194 To determine the stable carbon and hydrogen isotope composition of CH_4 ($\delta^{13}C_{CH4}$, $\delta^{2}H_{CH4}$), extracted
195 gas samples were first diluted to near-atmospheric CH_4 concentrations with synthetic air. Diluted
196 samples were then analysed on an automated IRMS system (Brass and Röckmann, 2010; Röckmann
197 et al., 2016) with a typical precision of <0.1‰ for $\delta^{13}C_{CH4}$ and <2‰ for $\delta^{2}H_{CH4}$. The system has been
198 validated in international intercomparison programs (Umezawa et al., 2018). The CO_2 isotopic
199 composition was determined using a modified system that had originally been designed for CO
200 isotopic analysis (Pathirana et al., 2015). In CO_2 analysis mode, a small amount of gas is admitted to
201 the system and the Schütze reagent used to oxidize CO to CO_2 is by-passed, allowing the
202 straightforward determination of $\delta^{13}C$ in CO_2. The system has been linked to international isotope
203 scales using reference cylinders prepared by the Max-Planck Institute for Biogeochemistry in Jena,
204 Germany. Multiple samples from the same soil-gas site have been analysed (Table S3). Bulk CH_4
205 and CO_2 isotopic ratios are expressed as permil vs. the Vienna Peedee Belemnite (VPDB) standard
206 for C and the Vienna Standard Mean Ocean Water (VSMOW) standard for H.
207
208 *3.3.3 CH_4 clumped-isotopes.*
209 For the clumped isotope analysis, CH_4 was separated from bulk gas and purified using a self-built
210 High Concentration Extraction System (HCES) (Sivan et al., 2023). In the first step, the complete
211 sample mixture is cryogenically collected on silica gel. Individual components are then separated on
212 packed gas chromatographic columns (a 5m long 1/4'' OD 5A molecular sieve column and a 2 m
213 long 1/4'' OD HayeSep D column) at 50°C using He as the carrier gas at a flow rate of 30 mL/min,
214 after which purified CH_4 is again collected on silica gel. Sample amounts are chosen based on prior

information for CH_4 content to yield 4 mL of pure CH_4, which is required for the high-precision clumped isotope analysis. The clumped isotopic composition of extracted CH_4 was analysed using a Thermo Ultra high-resolution IRMS. The typical measurement precision of a single measurement is 0.3‰ for $\Delta^{13}CH_3D$ and 2‰ for $\Delta^{12}CH_2D_2$. Multiple purifications of laboratory gas mixtures yielded results within these error estimates, indicating that the overall analytical procedure does not induce variability beyond instrumental errors. The long-term reproducibility of the mass spectrometer is around 0.3‰ for $\Delta^{13}CDH_3$ and 1.7‰ for $\Delta^{12}CD_2H_2$. To link the theoretical temperature calibration scale, isotope exchange experiments at various temperatures were performed using the laboratory reference gas. CH_4 was equilibrated at temperatures ranging from 50 to 450°C using two different catalysts: γ-Al_2O_3 for temperatures below 200°C and Pt on Al_2O_3 for 200-450°C. The experimental setup and subsequent calculations are thoroughly explained in Sivan et al., (2023).

3.3.4 CH_4 and CO_2 radiocarbon (^{14}C) and $\delta^{13}C$ analyses.

CH_4 and CO_2 were extracted from the four high-CH_4 soil-gas samples (i.e., P1, P8, A14, and A15, see Table 1) at the Laboratory for the Analysis of Radiocarbon (LARA), University of Bern, Switzerland, using an Acceleration Mass Spectrometry (AMS), with a methane preconcentration and purification setup (Espic et al., 2019). Due to the high concentrations of CO_2 and CH_4 for the samples from P1, A14 and A15, 0.6-2 mL of sample could be directly and manually injected into the gas chromatograph (GC, 7890B, Agilent, USA). For the P8 sample, a preconcentration step was necessary. The GC was equipped with a purged packed inlet, a packed column (ShinCarbon ST 80/100, 2 mm ID, L = 2 m, Restek, USA) and a thermal conductivity detector (TCD). He (purity = 99.999%, Carbagas, Switzerland) was used as a carrier gas. The oven was kept at 40ºC for 4 min and then heated to 250ºC with a temperature ramp of +10ºC/min, followed by a final cleaning step at 280ºC for 3 minutes. The system was operated in constant pressure mode (20 psig), which caused a gradual decrease in the He carrier gas flow rate from 14 mL min^{-1} to 9 mL min^{-1} during heating. The carbon-containing gases CO, CH_4, and CO_2 were well separated from each other, eluting at 3.5 min,

8 min, and 13 min, respectively. Pure CH_4 and CO_2 were trapped at liquid nitrogen temperatures in individual traps filled with 0.4 g charcoal, transferred into 4 mm OD glass ampoules (for CH_4 after combustion to CO_2 in a flow oven at 950°C using copper oxide wires of 0.5 mm diameter, Elementar, Germany) and sealed for isotope measurements. Radiocarbon and $\delta^{13}C$ analyses were performed at LARA and at the Laboratory of Ion Beam Physics, ETH, Zürich, Switzerland, using a AMS MICADAS (MIni CArbon DAting System), equipped with a gas ion source (Ruff et al., 2007). Glass ampoules provided by LARA Bern were cracked in the gas inlet system, and the CO_2 was mixed with He to ~5%, transferred into a syringe, and then fed into the ion source using a constant gas flow. Raw $^{14}C/^{12}C$, as well as $^{13}C/^{12}C$ ratios, were converted into $F^{14}C$ and $\delta^{13}C$ values, respectively, by performing a blank subtraction, and a standard normalization and correction for isotope fractionations (only for $F^{14}C$) using ^{14}C-free CO_2 and CO_2 produced from the primary NIST standard oxalic acid II (SRM 4990C), respectively, that were applied as ~5% mixtures with He. Multiple samples from the same soil-gas site have been analysed (Table S3).

3.3.5 Microbiological analysis of soil samples.

Forty soil samples from seven drilling points were collected at multiple depths ranging from 10 to 105 cm below the ground's surface. Five samples were obtained within two zones with high CH_4 concentrations (P1 and P8). Two samples were obtained at control sites, where CH_4 was not detected (at the time of soil sampling). Soil conditions are described in the Supplementary Material. To identify the presence and abundance of methanogens, the methyl coenzyme M reductase A genetic determinant (*mcrA*) was quantified using RealTime Polymerase Chain Reaction, PCR). We extracted DNA and amplified two types of gene targets via PCR: the first target, (16S) encoding the small protein subunit of the ribosome, is universally used to quantify total bacterial communities, while the second target, *mcrA*, is specific for methanogens. Three replicates for each of the genes were performed. Total DNA was extracted from 0.25 g of dried soil using the Qiagen DNeasy PowerSoil kit as described by the manufacturer. Extracted DNA was quantified with a Qubit 3.0 fluorimeter

(Thermo Fisher Scientific, USA) using the Qubit™ DNA HS Assay Kit (Thermo Fisher Scientific) and stored at -20°C. RealTime qPCR was performed by a QuantStudio 5 system (Life Technologies, USA). The qPCR reaction volume was equal to 5 µL, 1 µL of purified DNA solution and 4 µL of reaction mix, composed using 1.2 µL of PCR-grade water, 0.15 µL each of F and R primers (Table S5), and 2.5 µL of Power SYBR Green PCR Master Mix with Taq polymerase (Applied Biosystems, USA). qPCR thermal conditions were set to a pre-denaturing stage at 95°C for 10 minutes, followed by 40 cycles with a denaturation step at 95°C for 15 sec, an annealing step at 57°C for 60 sec, and an extension at 72°C for 60 sec. For each amplification, a negative control of sterile MilliQ water was run with three replicates.

4. Results

4.1 H_2, CH_4, and CO_2 concentrations in soils

We observed, both in the Pusteria and Anterseva valley, that H_2 was typically coupled to high CH_4 and CO_2 concentrations (Table S2). During the first survey, H_2 was detected at 106 points (43% of measured points), with concentrations ranging from 10 to 610 ppmv. In September 2021, at the P1 site, H_2 reached 1,700 ppmv (Fig. 1; Fig. S1), with 14 vol.% CH_4 and 27 vol.% CO_2. At site A14, H_2 reached 10,000 ppmv (CH_4 reached 51 vol.% and CO_2 reached 15.5 vol.%). Repeated analysis at site A14 (point 14a in Table S2) indicated a peak, with H_2 sensor saturation at 5 vol.% (although the signal rapidly decreased and is not reported within the data table). The second and third surveys confirmed three sites with the highest H_2-CH_4-CO_2 concentrations (P1, P8, and A14) and revealed an additional gas-rich site (A15, near the Salomone spring). Repeated measurements at the same soil-gas probe position revealed that H_2 concentrations frequently decreased over time, suggesting a limited amount of gas available within intercepted aerated soil layers (see "Intercomparison of H_2 sensors in the Supplementary Material). Interestingly, gas-rich soils (P1, P8, and, especially, A14 and

A15) were the only sites where H_2S was also detected (up to 200 ppmv, sensor upper range limit, at A14).

The spatial distribution of soil-gas H_2, compared with that of CO_2 (interpolation of the July 2021 survey data), is shown in Fig. 2. The H_2 distribution only partially coincides with two fault lineaments, the Pusteria Fault (PF) and the Kalkstein-Vallarga Fault (KV) (described in Supplementary Material). H_2 concentrations exceeding 100 ppmv also occurred far from fault zones.

Figure 2

4.2 Isotopic and radiocarbon composition CH_4 and CO_2

The stable C and H isotope composition of CH_4 at the four H_2-rich sites is reported in Table 1 and Fig. 3. The values are typical of microbial methanogenesis in peatlands and wetlands (Whiticar, 1999). The ^{13}C-enriched CH_4 of P1 (-41.6 ‰; Table 1) is coupled to a relevant concentration of slightly ^{13}C-enriched CO_2 (up to 27 vol.% detected on-site; $\delta^{13}C_{CO2}$: -17.9 ‰, which is within the range of the isotopic composition of CO_2 in freshwater environments; Whiticar, 1999; Figure 3). The radiocarbon content of CH_4 in all four sites ($F^{14}C > 1$; Table 1) confirmed modern microbial origin. The paired CH_4 clumped isotopes ($\Delta^{12}CH_2D_2$ - $\Delta^{13}CH_3D$) of CH_4 measured at P1 and A15 are in thermodynamic disequilibrium (Fig. 3B), which is typical of CH_4 generated via microbial pathways at relatively low temperatures (Young et al., 2017; Sivan et al., 2023). CO_2 at all four H_2-rich sites is also modern ($F^{14}C$: 0.8 to >1; Table 1).

Figure 3

Figure 4

4.3 Gas flux measurements

The CH_4 and H_2 flux measurements by closed-chamber technique performed in 5 points at the P1 (Pusteria Valley) and A14 (Anterselva Valley) sites (Figures 1 and S1) did not show any exhalation of the two gases. No gas concentration build-up was recorded within the chamber. Three measurements showed a negative CH_4 flux (-4, -4 and -5 mg m^{-2} day^{-1}), indicating methanotrophic consumption.

4.4 Analysis of gaseous hydrocarbons heavier than methane.

C_{2+} volatile hydrocarbons (ethane, propane, butane, pentane, and hexane) in the four, high-CH_4 soil-gas samples were below the FTIR detection limit of 1 ppmv (Table S4).

4.5 Analysis of H_2 and CH_4 dissolved in spring waters

In the five springs along the Pusteria and Anterselva Valleys (Fig. 1), CH_4 concentrations were always in equilibrium with the atmosphere, and H_2 concentrations were below detection limits (1.5-2 ppmv CH_4 and 5 ppmv H_2 within the extracted head-space, respectively).

4.6 DNA and mcrA gene quantitative polymerase chain reaction –qPCR- analyses

The microbiological analyses, performed on 40 soil samples from seven drilling points, clearly indicate that CH_4-rich sites (P1 and P8) host higher amounts of methanogenic bacteria as compared to the two control (no CH_4) sites (P1-BG and P8-BG) (Table S6). As expected, the quantity of methanogens initially increased with depth following lower redox potential. However, at approximately 40-60 cm the increase was attenuated and a decrease occurred, likely due to overall harsher conditions. At one of the richest CH_4 sites (P8b), the highest concentration of active bacteria was shallower (30 cm) than for the other sites.

5. Discussion

5.1 Multiple isotopic analyses unveiled a modern microbial origin for CH_4 and CO_2

The bulk isotopic composition of CH_4 and CO_2 suggest a biological origin of these gases (Figures 3 and 4). The ^{13}C-enrichment of CH_4 at P1 ($\delta^{13}C$: -41.6 ‰) could be related to substrate depletion or oxidation (Whiticar, 1999). Although oxidation is commonly observed at shallow depths above water-logged sediments (e.g., Hornibrook et al. 1997), there is no corresponding ^{2}H-enrichment in P1 (Fig. 3). Overall, the isotopic CH_4 and CO_2 data were compatible to signatures of methyl-fermentation (Fig. 4; Whiticar, 1999). The radiocarbon content of CH_4 and CO_2 in all four CH_4-CO_2-rich sites ($F^{14}C > 1$) confirmed modern microbial origin. Accordingly, an attribution to the overlapping abiotic genetic field in the clumped isotope diagram (Fig. 3B) is excluded. Therefore, the observed CH_4 is not a geological carrier of H_2.

The radiocarbon data represent a key finding because they clarifies that H_2 is only associated with modern microbial gases, which are all typical of fermentation. Since methanogens may thrive on any type of H_2, microbial CH_4 alone does not allow us to exclude a geological origin for H_2; but the presence of microbial CO_2 corroborates an exclusion because it is typically co-produced with H_2 during acetogenesis (Ye et al. 2014).

Understanding specific CH_4 and CO_2 sources, and potential isotopic C fractionation in the soil, was beyond the scope of this study; such an undertaking requires gas and organic matter ^{14}C analyses at multiple depths (e.g. Wordell-Dietrich et al. 2020). The unequivocal isotopic data demonstrated that microbial and modern CH_4 and CO_2 can reach elevated concentrations in aerated soil (up to >50 vol.% CH_4 and >20 vol.% CO_2). Similar CH_4 and CO_2 concentrations are common in landfill soils, where waste is decomposed by aerobic methanogenesis. However, we were unable to locate any reports of such high levels of microbial gas in natural aerated soils.

Whether or not the observed large quantities of CH_4 (up to 51 vol.%) were totally or partially produced in aerated soil portions (using CO_2 and H_2 migrating from fermentation sites) remains

undetermined. Methanogenesis in the aerated soils is a known process: as in our case, it was reported around wetlands (Angle et al. 2017) and in Tyrol Alpine soils (Hofmann et al., 2016). Due to the inherent reversibility of hydrogenase-encoding enzymes, leading to either the emission or consumption of H_2, depending on fluctuating metabolic requirements (Ogata and Lubitz, 2021), the detection of specific H_2 producing bacteria remained elusive. Nevertheless, the overall bacterial population (universal for the 16S ribosomal gene), which was several orders of magnitude higher than the methanogenic population, was particularly high at the P1 site. Therefore, it is possible that such an extra population included H_2 producers. H_2-generating metabolism is widespread across very diverse prokaryotic groups, and encompasses anaerobic gram positives, enterobacteria, symbiotic or free-living nitrogen-fixing bacteria, photosynthetic cyanobacteria, and sulphur bacteria.

5.2 No evidence of crustal degassing

H_2 and tectonic faults. The Pusteria Valley develops along a regional fault system, but the spatial distribution of soil-gas H_2, derived by interpolation of the July 2021 survey data (Fig. 2), only partially coincides with two fault lineaments, the Pusteria Fault (PF) and the Kalkstein-Vallarga Fault (KV) (see Supplementary Material). The P1 H_2-rich site, located near the PF trace, actually hosts high concentrations of microbial modern CO_2, which obviously is not a result of fault degassing (Fig. 2). Rather than faults, H_2 and CO_2 appear to generally follow the valley slope and bottom, which include flat areas, channels and depressions. These are zones of low relative elevation, inducing water accumulation, shallow groundwater flows, and increased soil moisture, factors that contribute to near-surface microbial gas production (e.g., Morozumi et al. 2019). Further ^{14}C analyses should be performed in other soil-gas sites along the PF to unambiguously identify possible geological degassing processes.

No gas exhalation to the atmosphere. Dry soil is known to be a net sink of H_2, with rapid H_2 consumption corroborated by negative fluxes (Conrad, 1996; Hammer and Levin, 2009; Chen et al., 2015). The presence of advective exhalation of H_2 from the soil to the atmosphere is, therefore,

396 considered to be a potential proxy for subsurface gas migration (Etiope, 2023). The flux
397 measurements of CH_4 and H_2 obtained using the closed-chamber technique within the richest gas
398 sites during September 2021 (Fig. 1) did not show the presence of active seepage. Gas concentrations
399 within the chamber were monitored over a five-minute interval, an interval that, with the specific
400 chamber-sensor system used, is generally sufficient to detect fluxes typical of active seeps (Etiope et
401 al. 2017; Etiope, 2023). The measurements suggest that the CH_4-H_2 concentrations within the soil are
402 not due to active, pressure-driven gas migration (seepage). High gas concentrations in soil pores
403 associated with a lack of fluxes to the atmosphere are more frequently related to small, low-pressure
404 pockets of *in situ* originated gas (Forde et al. 2018; Etiope, 2023). Despite the possibility that silty
405 material and wet layers may restrict the gas flow above the soil-gas sample depth (60–80 cm), the
406 negative CH_4 flux observed in three locations, which suggests methanotrophic consumption, typical
407 of dry soil, still points to the presence of air movement in the upper soil layers.
408 *No heavier hydrocarbons in soils and no geological gas in springs*. The lack of gaseous hydrocarbons
409 heavier than methane in the soil, which may be produced in deep C-rich rocks either by thermogenesis
410 or abiotic processes (Etiope and Sherwood Lollar, 2013), and the absence of H_2 associated with CH_4
411 in atmospheric equilibrium in the several springs, are additional indicators that the investigated
412 Alpine valleys do not host an appreciable crustal degassing. Other springs in the valleys did not have
413 any features that may suggest deep geothermal or serpentinization processes (no bubbling; pH < 9;
414 https://geoportale.retecivica.bz.it/geodati.asp). There were also no manifestations of gas seepage
415 within the area (no mofettes, no vegetation stress).
416
417 *5.3. Microbiological activity in the soil*
418 Although a large methanogenic population was detected in the investigated soils, whether or not the
419 observed large quantities of CH_4 (up to 51 vol.%) were totally or partially produced in aerated soil
420 portions (using CO_2 and H_2 migrating from fermentation sites) remains undetermined.
421 Methanogenesis in the aerated soils is a known process: as in our case, it was reported around

wetlands (Angle et al. 2017) and in Tyrol Alpine soils (Hofmann et al., 2016). Due to the inherent reversibility of hydrogenase-encoding enzymes, leading to either the emission or consumption of H_2, depending on fluctuating metabolic requirements (Ogata and Lubitz, 2021), the detection of specific H_2 producing bacteria remained elusive. Nevertheless, the overall bacterial population (universal for the 16S ribosomal gene), which was several orders of magnitude higher than the methanogenic population, was particularly high at the P1 site. Therefore, it is possible that such an extra population included H_2 producers. H_2-generating metabolism is widespread across very diverse prokaryotic groups, and encompasses anaerobic gram positives, enterobacteria, symbiotic or free-living nitrogen-fixing bacteria, photosynthetic cyanobacteria, and sulphur bacteria.

5.4 Potential biogenic sources of H_2 and CO_2

Although it can be hypothesized that methanogenic activity in the meadows could have been caused by crustal H_2 degassing (where bacteria use geological H_2 as an energy source), the simultaneous presence of high quantities of microbial CO_2 and H_2S is indicative of fermentation activity. CO_2, H_2S, and H_2 are, in fact, all typical co-products of two stages of anaerobic digestion, acetogenesis (the transformation of alcohols, and carbonic and fatty acids into gases) and, subordinately, acidogenesis (the conversion of sugars and amino acids; Valdez-Vazquez and Poggi-Varaldo, 2009). H_2 is a key intermediate in anaerobic environments and these fermentation stages are particularly enhanced in wet soils (Ye et al. 2014). While it is known that methanogenesis can occur in aerated soils (Angle et al. 2017; Hoffmann et al, 2016), fermentation requires anoxic conditions. The ^{14}C content of CO_2 suggests that the C feedstock (organic matter) is approximately 1200-1400 years old at P8 ($F^{14}C_{CO2}$: 0.846) and younger, influenced by the bomb spike ($F^{14}C_{CO2}$: >1), at the other three sites. These data are typical of fermentation observed in wetlands, fens, bogs, and peat soils (Chanton et al. 2008; Trumbore et al. 1999). Although we can assume that normal soil respiration (a common process in aerobic soils, leading to CO_2 concentrations typically <1 vol.%) exists in all investigated sites, we hypothesize that the large quantities of CO_2 (up to 27 vol.%), observed at depths of 60-80 cm, are

allochthonous (as well as the associated H_2, CH_4 and H_2S), and migrated from shallow wet soil layers and/or adjacent water-logged strata (wetland, fens) that are widespread in Tyrol Alpine grasslands (Fig. 1; Hilpold et al. 2023). The A14 site is, in fact, located between two wetland zones (bogs; Fig. 1 and Fig. S1; Supplementary Material). The P8 and A15 sites are located near diffuse water-logged soils, and are likely impacted by the emergence of shallow groundwater (and by the spring in A15). High H_2 concentrations in the apparently dry meadows of P1 and other sites, such as n. 12 and 22, as observed in the September 2021 survey (Table S2), were less expected. We could not obtain specific information regarding the depth of local aquifers. However, we could not exclude the existence of substantial organic matter under anaerobic conditions at shallow depth, induced by near surface water flows (the meadows around P1 host drainage channels), as is typical of Alpine proglacial zones and hillslopes (e.g., Müller et al. 2022; Penna et al. 2015).

Delving into the particular microbiological and environmental factors that could contribute to the high amounts of H_2, CH_4, and CO_2 was beyond the purview of our study, since our goal was to exclusively figure out whether H_2 and associated gases are geological. Additional research is required to broaden the current understanding of the soil's capacity for H_2 production and syntrophic consumption (Piché-Choquette and Constant, 2019; Meinel et al. 2022). Oxygenation (H_2 was extracted from aerated soils) and H_2S (observed at the richest H_2 sites) are known to be strong inhibitors of H_2 consumption. These and other potential inhibitors, such as organic acids and alcohols (Oremland and Taylor, 1975; Hoeler et al. 1998; Schmidt et al. 2016), will be considered in future studies. Studying the variation of H_2 with depth within the soil (as suggested in Zgonnik et al., 2015) could also be considered in a future work, but in our case this approach may not be effective in determining the source of H_2: in fact, in the vadose zone H_2 may increase with depth either if the gas migrates from deeper geological formations or is generated in moist subsoil and aquifers. Geological seepage could potentially be detected exclusively through boreholes that penetrate the bedrock beneath aquifers, on the condition that artificial H_2 production associated with drilling (as documented in Halas et al. 2021) can be disregarded.

5.5 Geological or biological H_2?

Table 2 summarizes multiple indicators, considered in this work, which may suggest a geological or biological origin for the H_2 observed within the Pusteria and Anterselva Valleys. No single indicator unequivocally demonstrates that H_2 is geological. Microbial origin is, instead, supported by multiple lines of evidence. The ^{14}C-enrichment of CO_2 is, in particular, a strong indication that H_2 is also microbial. While methanogenesis near the surface may develop through the use of geological H_2, modern CO_2 is compatible with acetogenesis during fermentation, for which H_2 and H_2S (the latter was observed at high CH_4-H_2-CO_2 sites) are typical products (i.e. Ye et al. 2014). The existence of geological H_2 degassing at sites dominated by microbial gas would be a tremendous coincidence. The coexistence of crustal helium (^4He) anomalies and hydrogen in the soil was suggested as a crucial element in determining the deep source of hydrogen, hence minimizing the possibility of misinterpreting surface biological hydrogen detection (e.g., Prinzhofer et al. 2024). Nevertheless, this concept is valid only if the potential ^4He radiogenic source rocks, such as granite basement and intrusions, are quite deep (e.g., within sedimentary basins). It is well known that in areas with shallow or outcropping crystalline basement, crustal helium in soil-gas is not a deep gas tracer, but it reflects groundwater circulation in fractured igneous rocks at shallow depths (e.g., Gregory and Durrance, 1987; Gascoyne et al. 1993). Therefore, detecting ^4He soil-gas anomalies in the Pusteria region, where the Australpine crystalline basement is exposed (Supplementary Material), may not be conclusive. Mantle-derived ^3He is virtually absent in near-surface groundwaters of the Central and Eastern Alps (Marty et al. 1992).

6. Conclusions

The results of this work suggest that aerated soils may host considerable amounts of microbial H_2, as observed for CH_4. This phenomenon should be considered in surface H_2 exploration guidelines. Caution should, then, be paid when interpreting concentrations of H_2 in the soil in the order of 10^2-10^3 ppmv, as in the case of the so-called "fairy circles" or "sub-circular depressions", which may host wet ground. Cursorily attributing a geological origin to H_2 in the soil, without a rigorous analysis of the isotopic composition of the associated gases, can be misleading. We demonstrated that radiocarbon analysis of CH_4 and CO_2 is a decisive interpretative tool.

The detected concentrations of microbial CH_4 and CO_2 also appear to be the highest ever reported in the scientific literature for aerated soils. In this respect, our study represents a new reference for the potential of microbial C-bearing gas production and greenhouse-gas cycle in surface environments. Future research should address the biological reasons for the high H_2 levels, and related modern CO_2 and CH_4, focusing on the potential H_2 consumption inhibitors, such as oxygen, sulphide, organic acids and alcohols. Acquiring further soil-gas and flux data in aerated and wet soils will be beneficial not only for improving natural CH_4 emission estimates, but also for expanding the dataset of surface biological H_2 generation, an essential baseline for the ongoing geological and geochemical exploration of natural hydrogen.

Data availability.

All data acquired in this study are available in this paper and Supplementary data file.

Declaration of competing interests

The authors declare no competing interests or personal relationships that could have appeared to influence the work reported in this paper.

Acknowledgements

We acknowledge support from the Istituto Nazionale di Geofisica e Vulcanologia ("Sezione Roma 2 - Etiope" project funds) and the Project SID (Investimento Strategico di Dipartimento) 2021 of University of Padova. M. Sivan and the Thermo Ultra instrument are supported by the Netherlands Earth Science System Center (NESSC), funded by the Ministry of Education, Culture and Science (OCW) and Utrecht University. We thank C. van der Veen for the isotopic analyses at Utrecht University. R. Conrad, C. Vogt, and M.E. Popa offered

fruitful discussions on biological H_2 production. A. Tondello is gratefully acknowledged for assistance in the DNA amplification analyses and P. Stevanato for the availability of required facilities. We also thank L. Ruggiero for help with soil sampling.

Author contributions. GE designed the multidisciplinary study, executed field measurements and laboratory FTIR analyses, interpreted all data, and developed the manuscript. GC, EB, RS and CM executed field measurements, contributed to geological analysis and mapping. TR and MS performed methane bulk and clumped isotope analyses. AS performed the microbiological analyses. TL, SS and NH performed the ^{14}C analyses. All authors contributed to data interpretation and manuscript refinement.

Supplementary Material

Supplementary text, figures and tables are annexed to this paper.

References

Angle, J.C., Morin, T.H., Solden, L.M., Narrowe, A.B., Smith, G.J., Borton, M.A., et al. (2017). Methanogenesis in oxygenated soils is a substantial fraction of wetland methane emissions. Nature Comm., 8, 1567, doi.org/10.1038/s41467-017-01753-4.

Benà, E., Ciotoli, G., Ruggiero, L., Coletti, C., Bossew, P., Massironi, M., et al. (2022). Evaluation of tectonically enhanced radon in fault zones by quantification of the radon activity index. Scientific Reports, 12, 21586.

Boreham, C.J., Edwards, D.S., Czado, K., Rollet, N.,Wang, L., van der Wielen, S., et al. (2021). Hydrogen in Australian natural gas: occurrences, sources and resources. The APPEA J., 61, 63-91.

Brass, M., Röckmann, T. (2010). Continuous-flow isotope ratio mass spectrometry method for carbon and hydrogen isotope measurements on atmospheric methane, Atmos. Meas. Tech., 3, 1707-1721.

Carrillo Ramirez, A., Gonzalez Penagos, F., Rodriguez, G., Moretti, I. (2023). Natural H_2 emissions in Colombian ophiolites: first findings. Geosciences, 13, 358.

Chanton, J.P., Glaser, P.H., Chasar, L.S., Burdige, D.J., Hines, M.E., Siegel, D.I., Tremblay, L.B., Cooper, W.T. (2008). Radiocarbon evidence for the importance of surface vegetation on fermentation

564 and methanogenesis in contrasting types of boreal peatlands. Global Biogeoch. Cycles 22, GB4022,
565 doi:10.1029/2008GB003274.
566
567 Chen Q., Popa M.E., Batenburg A.M., Röckmann T. (2015). Isotopic signatures of production and
568 uptake of H_2 by soil. Atmos. Chem. Phys., 15, 13003-21.
569
570 Conrad, R. (1996). Soil microorganisms as controllers of atmospheric trace gases (H_2, CO, CH_4, OCS,
571 N_2O, and NO). Microbiol. Rev., 60, 609-640.
572
573 Conrad, R., Seiler, W. (1980) Contribution of hydrogen production by biological nitrogen fixation to
574 the global hydrogen budget. J. Geoph. Res., Oceans, 85(C10), 5493-5498.
575
576 Dunham, E.C., Dore, J.E., Skidmore, M.L. (2021). Lithogenic hydrogen supports microbial primary
577 production in subglacial and proglacial environments. PNAS, 118, e2007051117.
578
579 Espic, C., Liechti, M., Battaglia, M., Paul, D., Röckmann, T., Szidat, S. (2019). Compound-specific
580 radiocarbon analysis of atmospheric methane: a new preconcentration and purification setup.
581 Radiocarbon, 61, 1461-1476, doi.org/10.1017/RDC.2019.76.
582
583 Etiope, G. (2023). Massive release of natural hydrogen from a geological seep (Chimaera, Turkey):
584 gas advection as a proxy of subsurface gas migration and pressurised accumulations. Int. J. Hydrogen
585 Energy, 48, 9172-9184, doi.org/10.1016/j.ijhydene.2022.12.025.
586
587 Etiope, G., Doezema, L., Pacheco, C. (2017). Emission of methane and heavier alkanes from the La
588 Brea Tar Pits seepage area, Los Angeles. J. Geophys. Res. Atm., 122, 12,008-12,019. doi:
589 10.1002/2017JD027675.
590
591 Etiope, G., Oze, C. (2022). Microbial vs abiotic origin of methane in continental serpentinized
592 ultramafic rocks: a critical review and the need of a holistic approach. App. Geochem., 143, 105373,
593 doi.org/10.1016/j.apgeochem.2022.105373
594
595 Etiope, G., Sherwood Lollar, B. (2013). Abiotic methane on Earth. Rev. Geophys. 51, 276–299,
596 doi.org/10.1002/rog.20011.
597

598 Forde, O.N., Mayer, K.U., Cahill, A.G., Mayer, B., Cherry, J.A., Parker, B.L. (2018). Vadose zone
599 gas migration and surface effluxes after a controlled natural gas release into an unconfined shallow
600 aquifer. Vadose Zone, 17, 180033.
601
602 Frery, E., Langhi, L., Maison, M., Moretti, I. (2021). Natural hydrogen seeps identified in the north
603 Perth Basin, western Australia. Int. J. Hydrogen Energy, 46, 31158-73.
604
605 Gascoyne, M., Wuschke, D.M., Durrance, E.M. (1993). Fracture detection and groundwater flow
606 characterization using He and Rn in soil gases, Manitoba, Canada. Appl. Geochem., 8, 223-233.
607
608 Gaucher, E.C. (2020). New perspectives in the industrial exploration for native hydrogen. Elements
609 16, 8-9.
610
611 Geymond, U., Briolet, T., Combaudon, V., Sissmann, O., Martinez, I., Duttine, M., Moretti, I. (2023).
612 Reassessing the role of magnetite during natural hydrogen generation. Frontiers in Earth Science, 11,
613 1169356.
614
615 Gregory, R.G., Durrance, E.M. (1987). Helium in soil gas: a method of mapping groundwater
616 circulation systems in fractured plutonic rock. Appl. Geochem., 2, 11-23.
617
618 Halas, P., Dupuy, A., Franceschi, M., Bordmann, V., Fleury, J.M., Duclerc, D. (2021). Hydrogen
619 gas in circular depressions in South Gironde, France: Flux, stock, or artefact? App. Geochem., 127,
620 104928.
621
622 Hammer, S., Levin, I. (2009). Seasonal variation of the molecular hydrogen uptake by soils inferred
623 from continuous atmospheric observations in Heidelberg, southwest Germany. Tellus B: Chemical
624 and Physical Meteorology, 61, doi:10.1111/j.1600-0889.2009.00417.x.
625
626 Hilpold, A., Anderle, M., Guariento, E., Marsoner, T., Mina, M., Paniccia, C., Plunger, J., Rigo, F.,
627 Rüdisser J., Scotti, A., Seeber, J., Steinwandter, M., Stifter, S., Strobl, J., Suarez-Muñoz, M., Vanek,
628 M., Bottarin, R., Tappeiner, U. (2023). Biodiversity Monitoring South Tyrol - Handbook,
629 Bozen/Bolzano, Italy, Eurac Research, doi.org/10.57749/2qm9-fq40
630

631 Hinkle, M. (1994). Environmental conditions affecting concentrations of He, CO_2, O_2 and N_2 in soil
632 gases. Appl. Geochem. 9, 53–63.
633
634 Hoehler, T.M., Alperin, M.J., Albert, D.B., Martens, C.S. (1998). Thermodynamic control on
635 hydrogen concentrations in anoxic sediments. Geochim. Cosmoch. Acta, 62, 1745-1756.
636
637 Hofmann, K., Praeg, N., Mutschlechner, M., Wagner, A.O., Illmer, P. (2016). Abundance and
638 potential metabolic activity of methanogens in well-aerated forest and grassland soils of an alpine
639 region. FEMS microbiology ecology, 92(2), fiv171.
640
641 Hornibrook, E.R., Longstaffe, F.J., Fyfe, W.S. (1997). Spatial distribution of microbial methane
642 production pathways in temperate zone wetland soils: Stable carbon and hydrogen isotope evidence.
643 Geochim. Cosmoch. Acta, 61, 745-753.
644
645 IEA (2023). Global Hydrogen Review 2023, IEA, Paris https://www.iea.org/reports/global-
646 hydrogen-review-2023,
647
648 Kinnaman, F.S., Valentine, D.L., Tyler, S.C. (2007). Carbon and hydrogen isotope fractionation
649 associated with the aerobic microbial oxidation of methane, ethane, propane and butane. Geochim.
650 Cosmochim. Acta 71, 271–283.
651
652 Krämer, H., Conrad, R. (1993). Measurement of dissolved H_2 concentrations in methanogenic
653 environments with a gas diffusion probe. FEMS Microbiology Ecology, 12, 149-158.
654
655 Langhi, L., Strand, J. (2023). Exploring natural hydrogen hotspots: a review and soil-gas survey
656 design for identifying seepage. Geoenergy, 1, doi.org/10.1144/geoenergy2023-014.
657
658 Larin, N., Zgonnik, V., Rodina, S., Deville, E., Prinzhofer, A., Larin, V.N. (2015). Natural molecular
659 hydrogen seepage associated with surficial, rounded depressions on the European craton in Russia.
660 Nat. Resour. Res., 24, 369-383.
661
662 Lefeuvre, N., Truche, L., Donz., F.-V., Ducoux, M., Barr., G., Fakoury, R.-A., et al. (2021). Native
663 H_2 exploration in the western Pyrenean foothills. Geochemistry, Geophysics, Geosystems, 22,
664 e2021GC009917, doi.org/10.1029/2021GC009917

Lévy, D., Roche, V., Pasquet, G., Combaudon, V., Geymond, U., Loiseau, K., Moretti, I. (2023). Natural H_2 exploration: tools and workflows to characterize a play. Sci. Tech. Energ. Transition, 78, 27, doi.org/10.2516/stet/2023021

Marty, B., O'Nions, R.K., Oxburgh, E.R., Martel, D., Lombardi, S. (1992). Helium isotopes in Alpine regions. Tectonophysics, 206, 71-78.

Mathur, Y., Awosiji, V., Mukerji, T., Scheirer, A.H., Peters, K.E. (2023). Soil geochemistry of hydrogen and other gases along the San Andreas fault. Int. J. Hydrogen Energy, 50, 411-419.

McMahon, C.J., Roberts, J.J., Johnson, G., Edlmann, K., Flude, S., Shipton, Z.K. (2023). Natural hydrogen seeps as analogues to inform monitoring of engineered geological hydrogen storage. Geol Soc Spec Publ., 528, doi.org/10.1144/SP528-2022-5.

Meinel, M., Delgado, A.G., Ilhan, Z.E., Aguero, M.L., Aguiar, S., Krajmalnik-Brown, R., Torres, C.I. (2022). Organic carbon metabolism is a main determinant of hydrogen demand and dynamics in anaerobic soils. Chemosphere, 303, 134877.

Milkov, A.V. (2022). Molecular hydrogen in surface and subsurface natural gases: abundance, origins and ideas for deliberate exploration. Earth Sci. Rev., 104063.

Milkov, A.V., Etiope, G. (2018). Revised genetic diagrams for natural gases based on a global dataset of >20,000 samples. Org. Geochem. 125, 109–120.

Moretti, I., Geymond, U., Pasquet, G., Aimar, L., Rabaute, A. (2022). Natural hydrogen emanations in Namibia: field acquisition and vegetation indexes from multispectral satellite image analysis. Int. J. Hydrogen Energy, 47, 35588-607.

Morozumi, T., Shingubara, R., Suzuki, R., Kobayashi, H., Tei, S., Takano, S., et al. (2019). Estimating methane emissions using vegetation mapping in the taiga–tundra boundary of a north-eastern Siberian lowland. Tellus B: Chem. Phys. Meteor., 71(1), 1581004.

Müller, T., Lane, S.N., Schaefli, B. (2022). Towards a hydrogeomorphological understanding of proglacial catchments: an assessment of groundwater storage and release in an Alpine catchment. Hydrology and Earth System Sciences, 26(23), 6029-6054.

Newell, K.D., Doveton, J.H., Merriam, D.F., Gilevska, T., Waggoner, W.M., Magnuson, L.M. (2007). H_2-rich and hydrocarbon gas recovered in a deep Precambrian well in Northeastern Kansas. Nat. Resour. Res., 16, 277–292.

Ogata, H., Lubitz, W. (2021). Bioenergetics Theory and Components | Hydrogenases Structure and Function, Editor: J. Jez, Encyclopedia of Biological Chemistry III (Third Edition), Elsevier, 66-73.

Oremland, R.S., Taylor, B.F. (1975). Inhibition of methanogenesis in marine sediments by acetylene and ethylene: validity of the acetylene reduction assay for anaerobic microcosms. App. Microbiol., 30, 707-709.

Osselin, F., Soulaine, C., Fauguerolles, C., Gaucher, E. C., Scaillet, B., Pichavant, M. (2022). Orange hydrogen is the new green. Nature Geoscience, 15, 765-769.

Pal, D.S., Tripathee, R., Reid, M.C., Schäfer, K.V., Jaffé, P.R. (2018). Simultaneous measurements of dissolved CH_4 and H_2 in wetland soils. Environm. Monitor. Assess., 190, 1-11.

Pathirana, S.L., van der Veen, C., Popa, M.E., Röckmann, T. (2015). An analytical system for stable isotope analysis on carbon monoxide using continuous-flow isotope-ratio mass spectrometry, Atmos. Meas. Tech., 8, 5315-5324, 10.5194/amt-8-5315-2015.

Paulot, F., Paynter, D., Naik, V., Malyshev, S., Menzel, R., Horowitz, L.W. (2021). Global modeling of hydrogen using GFDL-AM4.1: Sensitivity of soil removal and radiative forcing. Int. J. Hydrogen Energy, 46, 13446-13460.

Penna, D., Mantese, N., Hopp, L., Dalla Fontana, G., Borga, M. (2015). Spatio-temporal variability of piezometric response on two steep alpine hillslopes. Hydrological Processes, 29, 198-211.

Piché-Choquette, S., Constant, P. (2019). Molecular hydrogen, a neglected key driver of soil biogeochemical processes. Appl. Environm. Microbiology, 85, e02418-18.

Prinzhofer, A., Cissé, C.S.T., Diallo, A.B. (2018). Discovery of a large accumulation of natural hydrogen in Bourakebougou (Mali). Int. J. Hydrogen Energy, 43, 19315–19326.

Prinzhofer, A., Moretti, I., Francolin, J., Pacheco, C., d'Agostino, A., Werly, J., et al. (2019). Natural hydrogen continuous emission from sedimentary basins: the example of a Brazilian H2-emitting structure. Int. J. Hydrogen Energy, 44, 5676-85.

Prinzhofer, A., Rigollet, C., Lefeuvre, N., Françolin, J., de Miranda, P.E.V. (2024). Maricá (Brazil), the new natural hydrogen play which changes the paradigm of hydrogen exploration. Int. J. Hydrogen Energy, 62, 91-98.

Rhee, T.S., Brenninkmeijer, C.A.M., Röckmann, T. (2006). The overwhelming role of soils in the global atmospheric hydrogen cycle. Atmos. Chem. Phys., 6, 1611–1625, doi.org/10.5194/acp-6-1611-2006.

Rigollet, C., Prinzhofer, A. (2022). Natural Hydrogen: a new source of carbon-free and renewable energy that can compete with hydrocarbons. First Break, 40, 78-84.

Röckmann, T., Eyer, S., van der Veen, C., Popa, M. E., Tuzson, B., et al. (2016). In situ observations of the isotopic composition of methane at the Cabauw tall tower site, Atmos. Chem. Phys., 16, 10469-10487, doi.org/10.5194/acp-16-10469-2016.

Ruff, M., Wacker, L., Gäggeler, H.W., Suter, M., Synal, H.-A., Szidat, S. (2007). A gas ion source for radiocarbon measurements at 200 kV. Radiocarbon, 49, 307-314, doi.org/10.1017/S0033822200042235.

Schmidt, O., Hink, L., Horn, M.A., Drake, H.L. (2016). Peat: home to novel syntrophic species that feed acetate- and hydrogen-scavenging methanogens. The ISME journal, 10, 1954-1966.

Sherwood Lollar, B., Onstott, T.C., Lacrampe-Couloume, G., Ballentine, C.J. (2014). The contribution of the Precambrian continental lithosphere to global H_2 production. Nature 516, 379–382. doi:10.1038/nature14017

766 Sivan, M., Röckmann, T., van der Veen, C., Popa, M.E. (2023). Extraction, purification, and clumped
767 isotope analysis of methane ($\Delta^{13}CDH_3$ and $\Delta^{12}CD_2H_2$) from sources and the atmosphere, EGUsphere,
768 1-35, 10.5194/egusphere-2023-1906.
769
770 Starkey, R.L., Wight, K.M. (1945). Anaerobic corrosion of iron in soil. American Gas Association,
771 New York, pp.108.
772
773 Sugimoto, A., Fujita, N. (2006). Hydrogen concentration and stable isotopic composition of methane
774 in bubble gas observed in a natural wetland. Biogeochemistry, 81, 33-44.
775
776 Sugisaki, R., Ido, M., Takeda, H., Isobe, Y., Hayashi, Y., Nakamura, N., et al. (1983). Origin of
777 hydrogen and carbon dioxide in fault gases and its relation to fault activity. J. Geol. 91, 239–258.
778
779 Trumbore, S.E., Bubier, J.L., Harden, J.W., Crill, P.M. (1999). Carbon cycling in boreal wetlands: a
780 comparison of three approaches. J. Geophys. Res., Atmospheres 104, D22, 27673-27682.
781
782 Umezawa, T., Brenninkmeijer, C. A. M., Röckmann, T., van der Veen, C., Tyler, S. C., Fujita, R.,
783 Morimoto, S., Aoki, S., Sowers, T., Schmitt, J., Bock, M., Beck, J., Fischer, H., Michel, S. E.,
784 Vaughn, B. H., Miller, J. B., White, J. W. C., Brailsford, G., Schaefer, H., Sperlich, P., Brand, W. A.,
785 Rothe, M., Blunier, T., Lowry, D., Fisher, R. E., Nisbet, E. G., Rice, A. L., Bergamaschi, P., Veidt,
786 C., Levin, I. (2018). Interlaboratory comparison of $\delta^{13}C$ and δD measurements of atmospheric CH_4
787 for combined use of data sets from different laboratories. Atmos. Meas. Tech. 11(2), 1207-1231,
788 doi.org/10.5194/amt-11-1207-2018.
789
790 Vacquand, C., Deville, E., Beaumont, V., Guyot, F., Sissmann, O., Pillot, D., Arcilla, C., Prinzhofer,
791 A. (2018). Reduced gas seepages in ophiolitic complexes: evidences for multiple origins of the H_2-
792 CH_4-N_2 gas mixtures. Geochem. Cosmochim. Acta 233, 437–461.
793
794 Valdez-Vazquez, I., Poggi-Varaldo, H.M. (2009). Hydrogen production by fermentative consortia.
795 Renewable and sustainable energy reviews, 13, 1000-1013.
796
797
798 Warr, O., Giunta, T., Ballentine, C.J., Sherwood Lollar, B. (2019). Mechanisms and rates of ^4He,
799 ^{40}Ar, and H_2 production and accumulation in fracture fluids in Precambrian Shield environments.

Chem. Geol. 530, 119322, doi:10.1016/j.chemgeo.2019.119322

Whiticar, M.J. (1999). Carbon and hydrogen isotope systematics of bacterial formation and oxidation of methane. Chemical Geology, 161, 291-314.

Wordell-Dietrich, P., Wotte, A., Rethemeyer, J., Bachmann, J., Helfrich, M., Kirfel, K., Leuschner, C., Don, A. (2020). Vertical partitioning of CO_2 production in a forest soil. Biogeosciences, 17, 6341–6356, doi.org/10.5194/bg-17-6341-2020.

Xiang, Y., Sun, X., Liu, D., Yan, L., Wang, B., Gao, X. (2020). Spatial distribution of Rn, CO_2, Hg, and H_2 concentrations in soil gas across a thrust fault in Xinjiang, China. Front. Earth Sci., 8, doi.org/10.3389/feart.2020.554924.

Ye, R., Jin, Q., Bohannan, B., Keller, J.K., Bridgham, S.D. (2014). Homoacetogenesis: a potentially underappreciated carbon pathway in peatlands. Soil Biology and Biochemistry, 68, 385-391.

Yedinak, E.M. (2022). The curious case of geologic hydrogen: assessing its potential as a near-term clean energy source. Joule, 6, 503-508.

Young, E.D., Kohl, I.E., Sherwood Lollar, B., Etiope, G., Rumble III, D., Li, S., Haghnegahdar, M. A., Schauble, E.A., McCain, K.A., Foustoukos, D.I., Sutclife, C., Warr, O., Ballentine, C.J., Onstott, T.C., Hosgormez, H., Neubeck, A., Marques, J.M., Pérez-Rodríguez, I., Rowe, A.R., LaRowe, D.E., Magnabosco, C., Yeung, L.Y, Ash, J.L., Bryndzia, L.T. (2017). The relative abundances of resolved $^{12}CH_2D_2$ and $^{13}CH_3D$ and mechanisms controlling isotopic bond ordering in abiotic and biotic methane gases. Geochim. Cosmochim. Acta 203, 235-264, doi.org/10.1016/j.gca.2016.12.041.

Zgonnik, V. (2020). The occurrence and geoscience of natural hydrogen: a comprehensive review. Earth Sci Rev., 203, 103140.

Zgonnik, V., Beaumont V., Deville E., Larin N., Pillot D., Farrell K.M. (2015). Evidence for natural molecular hydrogen seepage associated with Carolina bays (surficial, ovoid depressions on the Atlantic Coastal Plain, Province of the USA). Prog Earth Planet Sci., 2, 31.

Figure captions

Figure 1. Location map of soil-gas surveys and the richest H_2-CH_4-CO_2 sites within the Pusteria and Anterselva Valleys. All data are provided in Table S2. Springs where dissolved gas was examined: S- Salomone; C- Casanova Neuhaus; T- Teodone fountain; TM- Teodone Museum; G- San Giovanni. Faults: DAV- Deffereggen-Anterselva-Valles Fault (mylonitic zone); KV- Kalkstein-Vallarga Fault; PF- Pusteria Fault. Geology and faults are from Benà et al. (2022). Geological details are provided in the Supplementary Material. Wetland location was extracted from the WebGIS of the Bolzano Province (Geoportale Alto Adige, https://geoportale.retecivica.bz.it/geodati.asp).

Figure 2. **The spatial distribution of H_2 and CO_2 in soil-gas along the Pusteria Valley.** Contour lines were derived by Natural Neighbour interpolation of July 2021 soil-gas sampling points (black dots). Green stars refer to the H_2-CH_4-CO_2 rich sites, also observed in all successive soil-gas surveys. Diamonds indicate other sites with high H_2 and CH_4 concentration (up to 370 ppmv and 9000 ppmv, respectively) observed during September 2021. Map base is from Digital Elevation Model (DEM) with resolution of 2.5 m. Wetland zones (brown squares) and faults are as shown in Fig. 1.

Figure 3. The bulk (A) and clumped (B) CH_4 isotopic composition in H_2-enriched soil-gas samples of the Pusteria (P1, P8) and Anterselva (A14, A15) Valleys. Data from IMAU Lab (Table 1). CR: Carbonate Reduction; F: Fermentation. Genetic plots: A, after Milkov and Etiope, (2018); B, after Etiope and Oze, (2022). Microbial oxidation trend (red dashed arrow in A) based on the $\delta^{13}C_{CH4}$–$\delta^{2}H_{CH4}$ correlated variations with $\Delta H/\Delta C \sim 8–9$ (Kinnaman et al., 2007). ^{13}C-enrichment of P1 may reflect ^{13}C-enriched CO_2 (Table 1) and substrate depletion. Paired with the modern ^{14}C dating (Table 1), the bulk and clumped-isotopes signatures (within overlapping microbial-abiotic genetic zonation) are all attributable to microbial origin. Measurement uncertainties do not extend beyond symbol size.

Figure 4. The four H_2-rich samples, P1, P8, A14 and A15, within the combination of $\delta^{13}C_{CH4}$ and $\delta^{13}C_{CO2}$ for microbial gas. The carbon isotope partitioning trajectories resulting from both methanogenesis and oxidation processes are shown (redrawn from Whiticar, 1999). Isotopic data are from the LARA-ETH analyses of CO_2 and CH_4 executed in the same gas samples (Table S3).

Table captions

Table 1. Mean values of the isotopic composition of CH_4 (bulk, clumped, radiocarbon) and CO_2 (stable carbon and radiocarbon) at the four, H_2-rich soil-gas sampling sites. The complete dataset is reported in Table S3. Gas samples were collected at the same sampling points at different times (within 30 min) and analysed in two different laboratories (see Methods).

Table 2. A synopsis of indicators supporting a biological or geological origin for H_2 within the studied Alpine Valleys.

Graphical Abstract

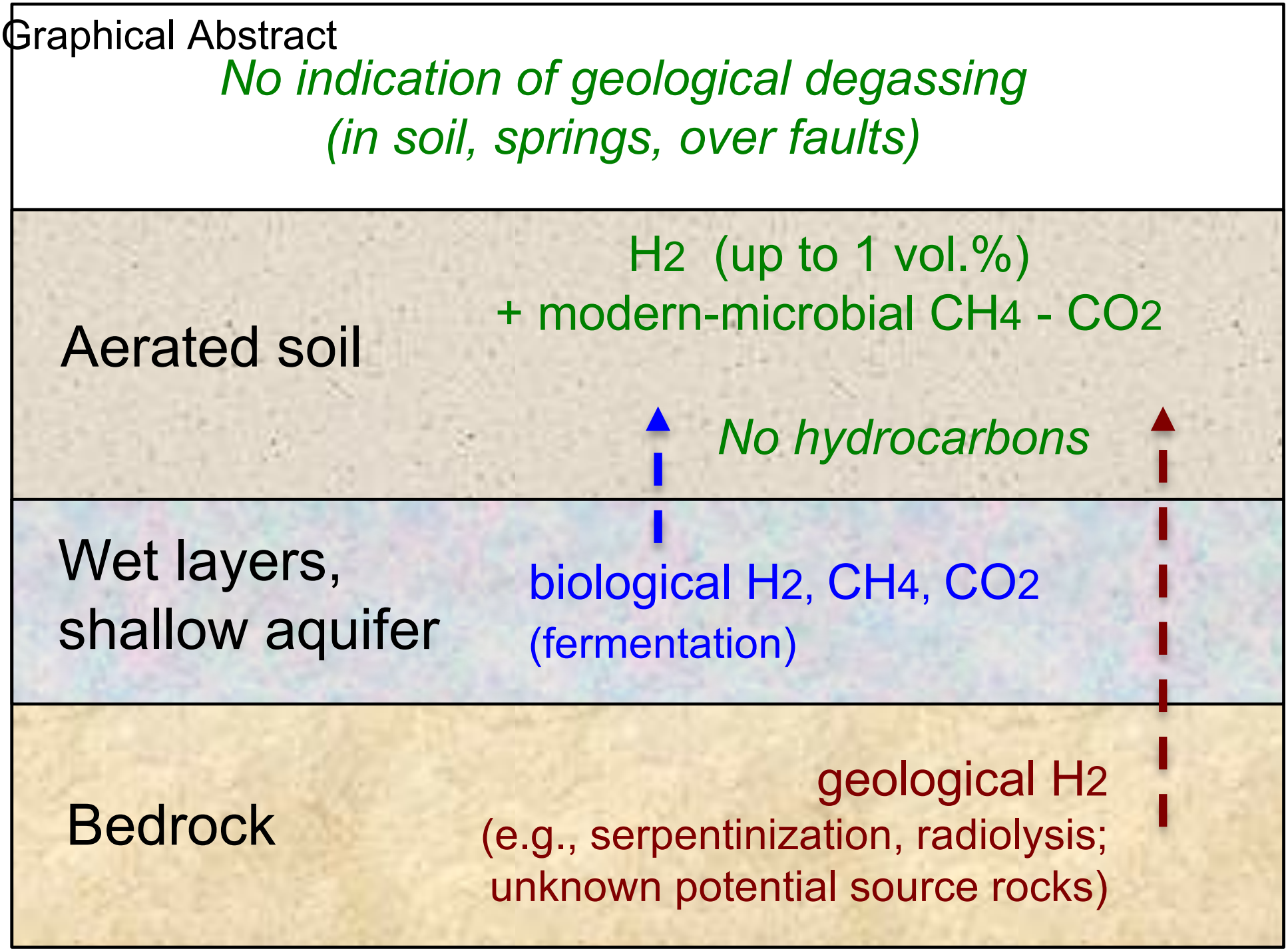

observations - *potential bio-source* - *potential geo-source*

Highlights

- High concentrations of H_2, CH_4 and CO_2 in soil resembling geological seepage
- Modern microbial CH_4 and CO_2 origin revealed by multiple isotopic analyses
- The highest concentrations of microbial CH_4 and CO_2 ever reported in aerated soils
- H_2 up to 1 vol.% in aerated soil may not necessarily be related to geological degassing
- Re-evaluation of the interpretation of H_2 in soils for natural hydrogen exploration

Surprising concentrations of hydrogen and non-geological methane and carbon dioxide in the soil

Etiope G.[1,2*], Ciotoli G.[3,1], Benà E.[4], Mazzoli, C.[4], Röckmann T.[5], Sivan M.[5], Squartini A.[6], Laemmel T.[7], Szidat S.[7], Haghipour N.[8], Sassi R.[4]

[1] *Istituto Nazionale di Geofisica e Vulcanologia, Sezione Roma2, Rome, Italy*
[2] *Faculty of Environmental Science and Engineering, Babes-Bolyai University, Cluj-Napoca, Romania*
[3] *Consiglio Nazionale delle Ricerche, Istituto di Geologia Ambientale e Geoingegneria, Monterotondo, Italy*
[4] *Dipartimento di Geoscienze, Università di Padova, Padova, Italy*
[5] *Institute for Marine and Atmospheric Research Utrecht, Utrecht University, The Netherlands*
[6] *Department of Agronomy, Food, Natural Res., Animals and Environment, Università di Padova, Padova, Italy*
[7] *Department of Chemistry, Biochemistry and Pharmaceutical Sciences & Oeschger Center for Climate Change Research, University of Bern, Bern, Switzerland*
[8] *Geological Institute & Laboratory of Ion Beam Physics, ETHZ, Zurich, Switzerland*
**Corresponding author: giuseppe.etiope@ingv.it*

Abstract

Due to its potential use as a carbon-free energy resource with minimal environmental and climate impacts, natural hydrogen (H_2) produced by subsurface geochemical processes is today the target of intensive research. In H_2 exploration practices, bacteria are thought to swiftly consume H_2 and, therefore, small near-surface concentrations of H_2, even orders of 10^2 ppmv in soils, are considered a signal of active migration of geological gas, potentially revealing underground resources. Here, we document an extraordinary case of a widespread occurrence of H_2 (up to 1 vol.%), together with elevated concentrations of CH_4 and CO_2 (up to 51 and 27 vol.%, respectively), in aerated meadow soils along Italian Alps valleys. Based on current literature, this finding would be classified as a discovery of pervasive and massive geological H_2 seepage. Nevertheless, an ensemble of gas geochemical and soil microbiological analyses, including bulk and clumped CH_4 isotopes, radiocarbon of CH_4 and CO_2, and DNA and *mcrA* gene quantitative polymerase chain reaction analyses, revealed that H_2 was only coupled to modern microbial gas. The H_2-CO_2-CH_4-H_2S association, wet soil proximity, and the absence of other geogenic gases in soils and springs suggest that H_2 derives from near-surface fermentation, rather than geological degassing. H_2 concentrations

up to 1 vol.% in soils are not conclusive evidence of deep gas seepage. This study provides a new reference for the potential of microbial H_2, CH_4 and CO_2 in soils, to be considered in H_2 exploration guidelines and soil carbon and greenhouse-gas cycle research.

Keywords: Natural hydrogen, methane, carbon dioxide, soil-gas, radiocarbon

1. Introduction

Natural hydrogen gas (H_2) produced by a variety of geochemical processes in crustal and mantle rocks is currently sought-after for its use as a carbon-free energy resource with low environmental and climate impacts (e.g., Gaucher, 2020; Rigollet and Prinzhofer, 2022; Yedinak, 2022). Together with artificially produced hydrogen (e.g., black/gray, blue, green hydrogen; IEA, 2023) and the hydrogen generation stimulated by geochemical reactions in the underground (orange hydrogen; Osselin et al. 2022), the naturally occurring geological H_2 (also referred to as "white" or "gold" hydrogen) might contribute to new hydrogen economy implementation. The geochemical processes generating subsurface H_2 are mostly related to water-rock reactions such as serpentinization (olivine hydration), radiolysis, and several types of iron oxidation (Sherwood Lollar et al. 2014; Warr et al. 2019; Zgonnik, 2020; Milkov, 2022; Geymond et al. 2023). Relevant amounts (up to 98 vol.%) of H_2 have been directly discovered in reservoirs intercepted by wells in the United States, Mali, Australia, and the Russian Federation (Newell et al 2007; Prinzhofer et al. 2018; Boreham et al. 2021; Zgonnik, 2020 and references therein). In other countries, H_2 is increasingly reported at the surface in soil or gas seeps (Zgonnik, 2020; Vacquand et al. 2018; Etiope, 2023; McMahon et al. 2023), and surface geochemistry is becoming part of global H_2 exploration (Lefeuvre et al. 2021; Frery et al. 2021; Lévy et al. 2023; Langhi and Strand, 2023). In soil-gas prospections, diffuse application of a paradigm exists by which H_2 microbially generated in wet soils and aquifers is rapidly consumed by bacteria and it should not occur in the aerated vadose zone (e.g., Rhee et al. 2006; Larin et al. 2015; Zgonnik

et al. 2015; Paulot et al. 2021). Therefore, the presence of H_2 in soil-gas, at concentrations on the order of 10^1-10^3 parts per million by volume (ppmv), is thought to be evidence of non-exogenous sources, i.e., geological degassing (seepage) from underground sources. This concept has been applied, for example, to so called "fairy circles" observed in Russia, the United States, Brazil, Australia, Namibia and Colombia (Larin et al. 2015; Zgonnik et al. 2015; Prinzhofer et al. 2019; Frery et al. 2021; Moretti et al., 2022; Carrillo Ramirez et al. 2023), to Pyrenean soils (Lefeuvre et al. 2021), to the San Andreas Fault in California (Mathur et al. 2023), and in proposed H_2 exploration guidelines (Lévy et al. 2023). However, similar amounts of H_2 can be produced by multiple microbially mediated processes, including fermentation in wet soils or shallow aquifers, N_2 fixation, and cellulose decomposition by termites (Conrad and Seilert, 1980; Krämer and Conrad, 1993; Sugimoto and Fujita, 2006; Pal et al. 2018), by the oxidation or corrosion of ferrous minerals (e.g., Starkey and Wight, 1945), and by the hydration of silicate radicals in basaltic soils (Dunham et al. 2021). Therefore, caution has been advised when cursorily attributing the term "seep" or "seepage" to soil-gas H_2 at ppmv levels (Etiope, 2023). H_2 may persist in soils due to inhibitors of syntrophic H_2 consumption such as hydrogen sulphide, alcohols, and organic acids (Hoeler et al. 1998; Schmidt et al. 2016; Meinel et al. 2022). The primary issue for understanding the H_2 potential in the soils is the paucity of available soil gas datasets. A few studies have focused on H_2 in soils as a tracer of faults and seismicity (e.g., Sugisaki et al., 1983; Xiang et al. 2020). Bio-ecosystem studies have largely addressed wetlands and the capacity of dry soil to act as an atmospheric H_2 sink, with a focus on laboratory tests and modelling, and without extensive *in situ* soil-gas surveys (e.g., Conrad 1996; Chen et al. 2015). As a result, insufficient data exists regarding background H_2 values, irrespective of soil moisture content or geological setting. Understanding the origin of H_2 in soil-gas is also complicated by the fact that biological and geological processes can produce H_2 with a similar isotopic composition ($^2H/H$, expressed as δ^2H), therefore, isotopic analyses may not be conclusive (Etiope, 2023). Given the issues outlined above, interpretations of H_2 origin should be based on a multidisciplinary, integrated study, including a compositional and isotopic analysis of the gases

86 associated with H_2. Careful investigations of the geology and the ecosystem are also necessary.
87 Here, we present an apparently straightforward case of relevant H_2 concentrations in aerated soils,
88 reaching 1 vol.%, which, based on current scientific literature, would immediately be classified as
89 the discovery of pervasive and massive geological H_2 seepage. The study was performed in two
90 valleys within the Eastern Alps (the Pusteria and Anterselva Valleys) of northern Italy, where high
91 H_2 values, associated with high methane (CH_4) values, were accidentally discovered in a previous
92 soil-gas survey addressed to radon. The H_2 and CH_4 data, not published in the radon study (Benà et
93 al. 2022), boosted the present study due to their noteworthy concentrations. Since elevated levels of
94 H_2 in aerated soils are commonly attributed to crustal degassing of geological origin (Larin et al.
95 2015; Zgonnik et al. 2015; Prinzhofer et al. 2019; Frery et al. 2021; Lefeuvre et al. 2021; Moretti et
96 al., 2022), our objective was to assess whether the high H_2 concentrations in the two Alpine valleys
97 are actually of geological origin or, rather, are a product of near-surface biological processes. To this
98 aim, we carried out an ensemble of gas geochemical and microbiological investigations (listed in
99 Table S1), including a wide soil-gas survey and multiple isotopic and radiocarbon analysis of CH_4
100 and CO_2 associated to H_2 in the soil. H_2 was also searched in several springs along the valleys. Surface
101 exploration of natural hydrogen has never made use of such an ensemble of analyses, particularly
102 radiocarbon analysis of CH_4 and CO_2 associated to H_2. Since the research was conceived as a surface
103 exploration of natural H_2 with the aim of understanding whether crustal degassing exists in the studied
104 area, investigating the specific biological and environmental elements that may have contributed to
105 the high levels of H_2 was beyond the scope of work. This study demonstrates the complexity of soil-
106 gas interpretations of H_2 and presents a crucial case to consider for future research and natural H_2
107 exploration guidelines.
108
109
110 **2. Geological setting of Pusteria and Anterselva valleys**
111

The Pusteria Valley develops along a segment of the Periadriatic lineament, the Pusteria Fault (PF), which is an East–West trending, a sub vertical aseismic fault with dextral transpressive strike-slip kinematics, representing the tectonic boundary between the Austroalpine crystalline basement to the north and the Southalpine basement to the south (Fig. 1; Schmid et al. 1989).

Figure 1

The Austroalpine crystalline basement in the Eastern Alps consists of pre-Variscan sequences. These were mainly affected by a Variscan (320-350 Ma) metamorphic event covering the whole temperature range of the amphibolite and greenschist facies at metamorphic thermal gradients of about 40°C/km, partly affected by Alpine metamorphic overprint (Sassi et al., 2004; Spiess et al., 2010). It is mainly made up by paragneisses and micaschists (locally grading to migmatites), in which orthogneisses, amphibolites, quartzites and marbles are interlayered. Eclogites, metabasites and metaultramafics locally occur. The Southalpine crystalline basement in the Eastern Alps consists of a thick phyllitic sequence affected by Variscan metamorphism under greenschist facies (Spiess et al. 2010). The Austroalpine block is cut by two major E-W trending tectonic lines: the DAV (Defferegger-Antholz/Anterselva-Vals/Valles fault (DAV) and the KV (Kalkstein-Vallarga) faults (Fig. 1). The DAV is a ~80 km long mainly mylonitic shear zone with dominant sinistral strike slip delimiting towards the south the Alpine metamorphic overprint (Müller et al. 2000). The KV is a transpressive strike-slip fault (Borsi et al., 1978). These two faults merge westwards close to the Insubric Line. Based on seismic reflectors, Lammerer et al. (2011) suggest the presence of schists containing serpentinites at depths of at least 5 km, in correspondence with the DAV and PF lineaments. The Anterselva Valley, is NNE-SSW oriented, was formed by glacial excavation along both the Austroalpine and Southalpine domains, and is crossed by the KV fault (Fig. 1). The soil features are described in the Supplementary Material.

3. Methods

3.1 Sampling and the on-site analysis of gas in soils.

Soil-gas surveys were conducted during July 2021 (244 sampling points) and September 2021 (89 points, using two different sensors for both H_2 and CH_4, described below, with multiple measurements surrounding the H_2-rich points observed in July 2021). A check of H_2 and CH_4 was repeated in August 2023 (16 points; Fig. 1 and Tables S1 and S2). In addition to the Pusteria Valley, soil-gas surveys included the adjacent N-S trending Anterselva Valley, transversally crossed by a fault (Fig. 1). Soil-gas sampling, conducted during July and September 2021, and August 2023 (Tables S1 and S2), was performed by pounding stainless-steel probes with a sliding hammer to depths of 60-80 cm. To minimize soil moisture, soil and air temperature and barometric pressure effects (Hinkle, 1994), sampling was performed over a very short period of time and during stable meteorological conditions. The probe was then connected to the following portable gas detectors, for measuring H_2, CH_4, CO_2, O_2, and H_2S:

H_2: (a) A Dräger electrochemical sensor (DrägerSensor® XXS H_2, Dräger X-am 7000, Germany; accuracy ≤1% of measured value; range 0-2000 ppmv) used during July and September 2021, and August 2023; (b) A Huberg semiconductor + pellistor sensor (Huberg Metrex 2, Italy; range 0-5 vol.%; accuracy ≤2% at 1000 ppmv, and ≤1% at 10,000 ppmv) used during September 2021. Further details and sensor intercomparison tests are reported in the Supplementary Material.

CH_4: (a) A Dräger infrared sensor (DrägerSensor® Smart IR CH_4, Dräger X-am 7000, Germany; accuracy: ≤5%; range 0.1-100 vol.%) used during July and September 2021, and August 2023; (b) A Tunable Diode Laser Adsorption Spectrometry (TDLAS) detector (Gazomat, France; precision 0.1 ppmv, lower detection limit 0.1 ppmv; range 0-100 vol.%) used during September 2021.

CO_2: (a) A Dräger infrared sensor (DrägerSensor® Smart IR CO_2 HC, Dräger X-am 7000, Germany; accuracy: ≤0.2%; range 0-100 vol.%) used during July and September 2021, and August 2023; (b) A Licor non-dispersive infrared sensor (Licor LI-820; accuracy <3% of reading; range 0-20,000 ppmv)

used during September 2021.

O_2: (a) A Dräger electrochemical sensor (DrägerSensor® XXS O_2, Dräger X-am 7000, Germany; accuracy: ≤0.2%; range 0-25 vol.%) used during July and September 2021, and August 2023.

H_2S: (a) A Dräger electrochemical sensor (DrägerSensor® XXS H_2S, Dräger X-am 7000, Germany; precision: 0.5 ppmv; range 0-200 ppmv) used during July and September 2021, and August 2023.

The spatial distribution of H_2 and CO_2 in soil-gas along the Pusteria Valley was derived by Natural Neighbour interpolation of July 2021 soil-gas sampling points, using Surfer 23.1.162 (copyright 1993–2021, Golden Software, LLC).

H_2 and CH_4 fluxes from soils were measured using a closed chamber technique in 5 points at the P1 (Pusteria Valley) and A14 (Anterselva Valley) sites (Figure S1). A 30cm-diameter static accumulation chamber was connected to the semiconductor H_2 and laser CH_4 sensors described above, using the same procedure in Etiope (2023) and Etiope et al (2017).

At sites P1, P8, A14, and A15, soil-gas samples were collected for the laboratory analyses described below. Gas was stored in evacuated Teflon bags and Wheaton bottles sealed with gas impermeable, thick, blue butyl septa (Bellco Glass Inc., NJ, USA) and aluminum crimp caps.

3.2 Sampling and the on-site analysis of gas dissolved in spring water.

CH_4 and H_2 were analysed in five spring water samples collected along the Pusteria and Anterselva Valleys (the spring name and location are reported in Fig. 1). Dissolved gas was extracted via an equilibration head-space method in 500 mL Duran bottles, and analysed using the TDLAS (for CH_4) and the semiconductor sensor (for H_2) described above.

3.3 Laboratory analyses of gas samples.

3.3.1 Analysis of C_2-C_6 hydrocarbons.

189 The presence of C_{2+} volatile hydrocarbons (ethane, propane, butane, pentane, and hexane) in the four,
190 high-CH_4 soil-gas samples, stored in Teflon bags, was checked by Fourier Transform Infrared
191 Spectroscopy (FTIR, Gasmet DX-4030, Finland; lower detection limit 1 ppmv, accuracy ±10%).
192
193 *3.3.2 CH_4 and CO_2 isotopic analyses.*
194 To determine the stable carbon and hydrogen isotope composition of CH_4 ($\delta^{13}C_{CH4}$, $\delta^{2}H_{CH4}$), extracted
195 gas samples were first diluted to near-atmospheric CH_4 concentrations with synthetic air. Diluted
196 samples were then analysed on an automated IRMS system (Brass and Röckmann, 2010; Röckmann
197 et al., 2016) with a typical precision of <0.1‰ for $\delta^{13}C_{CH4}$ and <2‰ for $\delta^{2}H_{CH4}$. The system has been
198 validated in international intercomparison programs (Umezawa et al., 2018). The CO_2 isotopic
199 composition was determined using a modified system that had originally been designed for CO
200 isotopic analysis (Pathirana et al., 2015). In CO_2 analysis mode, a small amount of gas is admitted to
201 the system and the Schütze reagent used to oxidize CO to CO_2 is by-passed, allowing the
202 straightforward determination of $\delta^{13}C$ in CO_2. The system has been linked to international isotope
203 scales using reference cylinders prepared by the Max-Planck Institute for Biogeochemistry in Jena,
204 Germany. Multiple samples from the same soil-gas site have been analysed (Table S3). Bulk CH_4
205 and CO_2 isotopic ratios are expressed as permil vs. the Vienna Peedee Belemnite (VPDB) standard
206 for C and the Vienna Standard Mean Ocean Water (VSMOW) standard for H.
207
208 *3.3.3 CH_4 clumped-isotopes.*
209 For the clumped isotope analysis, CH_4 was separated from bulk gas and purified using a self-built
210 High Concentration Extraction System (HCES) (Sivan et al., 2023). In the first step, the complete
211 sample mixture is cryogenically collected on silica gel. Individual components are then separated on
212 packed gas chromatographic columns (a 5m long 1/4'' OD 5A molecular sieve column and a 2 m
213 long 1/4'' OD HayeSep D column) at 50°C using He as the carrier gas at a flow rate of 30 mL/min,
214 after which purified CH_4 is again collected on silica gel. Sample amounts are chosen based on prior

information for CH_4 content to yield 4 mL of pure CH_4, which is required for the high-precision clumped isotope analysis. The clumped isotopic composition of extracted CH_4 was analysed using a Thermo Ultra high-resolution IRMS. The typical measurement precision of a single measurement is 0.3‰ for $\Delta^{13}CH_3D$ and 2‰ for $\Delta^{12}CH_2D_2$. Multiple purifications of laboratory gas mixtures yielded results within these error estimates, indicating that the overall analytical procedure does not induce variability beyond instrumental errors. The long-term reproducibility of the mass spectrometer is around 0.3‰ for $\Delta^{13}CDH_3$ and 1.7‰ for $\Delta^{12}CD_2H_2$. To link the theoretical temperature calibration scale, isotope exchange experiments at various temperatures were performed using the laboratory reference gas. CH_4 was equilibrated at temperatures ranging from 50 to 450°C using two different catalysts: γ-Al_2O_3 for temperatures below 200°C and Pt on Al_2O_3 for 200-450°C. The experimental setup and subsequent calculations are thoroughly explained in Sivan et al., (2023).

3.3.4 CH_4 and CO_2 radiocarbon (^{14}C) and $\delta^{13}C$ analyses.

CH_4 and CO_2 were extracted from the four high-CH_4 soil-gas samples (i.e., P1, P8, A14, and A15, see Table 1) at the Laboratory for the Analysis of Radiocarbon (LARA), University of Bern, Switzerland, using an Acceleration Mass Spectrometry (AMS), with a methane preconcentration and purification setup (Espic et al., 2019). Due to the high concentrations of CO_2 and CH_4 for the samples from P1, A14 and A15, 0.6-2 mL of sample could be directly and manually injected into the gas chromatograph (GC, 7890B, Agilent, USA). For the P8 sample, a preconcentration step was necessary. The GC was equipped with a purged packed inlet, a packed column (ShinCarbon ST 80/100, 2 mm ID, L = 2 m, Restek, USA) and a thermal conductivity detector (TCD). He (purity = 99.999%, Carbagas, Switzerland) was used as a carrier gas. The oven was kept at 40ºC for 4 min and then heated to 250ºC with a temperature ramp of +10ºC/min, followed by a final cleaning step at 280ºC for 3 minutes. The system was operated in constant pressure mode (20 psig), which caused a gradual decrease in the He carrier gas flow rate from 14 mL min^{-1} to 9 mL min^{-1} during heating. The carbon-containing gases CO, CH_4, and CO_2 were well separated from each other, eluting at 3.5 min,

8 min, and 13 min, respectively. Pure CH_4 and CO_2 were trapped at liquid nitrogen temperatures in individual traps filled with 0.4 g charcoal, transferred into 4 mm OD glass ampoules (for CH_4 after combustion to CO_2 in a flow oven at 950°C using copper oxide wires of 0.5 mm diameter, Elementar, Germany) and sealed for isotope measurements. Radiocarbon and $\delta^{13}C$ analyses were performed at LARA and at the Laboratory of Ion Beam Physics, ETH, Zürich, Switzerland, using a AMS MICADAS (MIni CArbon DAting System), equipped with a gas ion source (Ruff et al., 2007). Glass ampoules provided by LARA Bern were cracked in the gas inlet system, and the CO_2 was mixed with He to ~5%, transferred into a syringe, and then fed into the ion source using a constant gas flow. Raw $^{14}C/^{12}C$, as well as $^{13}C/^{12}C$ ratios, were converted into $F^{14}C$ and $\delta^{13}C$ values, respectively, by performing a blank subtraction, and a standard normalization and correction for isotope fractionations (only for $F^{14}C$) using ^{14}C-free CO_2 and CO_2 produced from the primary NIST standard oxalic acid II (SRM 4990C), respectively, that were applied as ~5% mixtures with He. Multiple samples from the same soil-gas site have been analysed (Table S3).

3.3.5 Microbiological analysis of soil samples.

Forty soil samples from seven drilling points were collected at multiple depths ranging from 10 to 105 cm below the ground's surface. Five samples were obtained within two zones with high CH_4 concentrations (P1 and P8). Two samples were obtained at control sites, where CH_4 was not detected (at the time of soil sampling). Soil conditions are described in the Supplementary Material. To identify the presence and abundance of methanogens, the methyl coenzyme M reductase A genetic determinant (*mcrA*) was quantified using RealTime Polymerase Chain Reaction, PCR). We extracted DNA and amplified two types of gene targets via PCR: the first target, (16S) encoding the small protein subunit of the ribosome, is universally used to quantify total bacterial communities, while the second target, *mcrA*, is specific for methanogens. Three replicates for each of the genes were performed. Total DNA was extracted from 0.25 g of dried soil using the Qiagen DNeasy PowerSoil kit as described by the manufacturer. Extracted DNA was quantified with a Qubit 3.0 fluorimeter

(Thermo Fisher Scientific, USA) using the Qubit™ DNA HS Assay Kit (Thermo Fisher Scientific) and stored at -20°C. RealTime qPCR was performed by a QuantStudio 5 system (Life Technologies, USA). The qPCR reaction volume was equal to 5 µL, 1 µL of purified DNA solution and 4 µL of reaction mix, composed using 1.2 µL of PCR-grade water, 0.15 µL each of F and R primers (Table S5), and 2.5 µL of Power SYBR Green PCR Master Mix with Taq polymerase (Applied Biosystems, USA). qPCR thermal conditions were set to a pre-denaturing stage at 95°C for 10 minutes, followed by 40 cycles with a denaturation step at 95°C for 15 sec, an annealing step at 57°C for 60 sec, and an extension at 72°C for 60 sec. For each amplification, a negative control of sterile MilliQ water was run with three replicates.

4. Results

4.1 H_2, CH_4, and CO_2 concentrations in soils

We observed, both in the Pusteria and Anterseva valley, that H_2 was typically coupled to high CH_4 and CO_2 concentrations (Table S2). During the first survey, H_2 was detected at 106 points (43% of measured points), with concentrations ranging from 10 to 610 ppmv. In September 2021, at the P1 site, H_2 reached 1,700 ppmv (Fig. 1; Fig. S1), with 14 vol.% CH_4 and 27 vol.% CO_2. At site A14, H_2 reached 10,000 ppmv (CH_4 reached 51 vol.% and CO_2 reached 15.5 vol.%). Repeated analysis at site A14 (point 14a in Table S2) indicated a peak, with H_2 sensor saturation at 5 vol.% (although the signal rapidly decreased and is not reported within the data table). The second and third surveys confirmed three sites with the highest H_2-CH_4-CO_2 concentrations (P1, P8, and A14) and revealed an additional gas-rich site (A15, near the Salomone spring). Repeated measurements at the same soil-gas probe position revealed that H_2 concentrations frequently decreased over time, suggesting a limited amount of gas available within intercepted aerated soil layers (see "Intercomparison of H_2 sensors in the Supplementary Material). Interestingly, gas-rich soils (P1, P8, and, especially, A14 and

A15) were the only sites where H_2S was also detected (up to 200 ppmv, sensor upper range limit, at A14).

The spatial distribution of soil-gas H_2, compared with that of CO_2 (interpolation of the July 2021 survey data), is shown in Fig. 2. The H_2 distribution only partially coincides with two fault lineaments, the Pusteria Fault (PF) and the Kalkstein-Vallarga Fault (KV) (described in Supplementary Material). H_2 concentrations exceeding 100 ppmv also occurred far from fault zones.

Figure 2

4.2 Isotopic and radiocarbon composition CH_4 and CO_2

The stable C and H isotope composition of CH_4 at the four H_2-rich sites is reported in Table 1 and Fig. 3. The values are typical of microbial methanogenesis in peatlands and wetlands (Whiticar, 1999). The ^{13}C-enriched CH_4 of P1 (-41.6 ‰; Table 1) is coupled to a relevant concentration of slightly ^{13}C-enriched CO_2 (up to 27 vol.% detected on-site; $\delta^{13}C_{CO2}$: -17.9 ‰, which is within the range of the isotopic composition of CO_2 in freshwater environments; Whiticar, 1999; Figure 3). The radiocarbon content of CH_4 in all four sites ($F^{14}C > 1$; Table 1) confirmed modern microbial origin. The paired CH_4 clumped isotopes ($\Delta^{12}CH_2D_2$ - $\Delta^{13}CH_3D$) of CH_4 measured at P1 and A15 are in thermodynamic disequilibrium (Fig. 3B), which is typical of CH_4 generated via microbial pathways at relatively low temperatures (Young et al., 2017; Sivan et al., 2023). CO_2 at all four H_2-rich sites is also modern ($F^{14}C$: 0.8 to >1; Table 1).

Figure 3

Figure 4

4.3 Gas flux measurements

The CH_4 and H_2 flux measurements by closed-chamber technique performed in 5 points at the P1 (Pusteria Valley) and A14 (Anterselva Valley) sites (Figures 1 and S1) did not show any exhalation of the two gases. No gas concentration build-up was recorded within the chamber. Three measurements showed a negative CH_4 flux (-4, -4 and -5 mg m^{-2} day^{-1}), indicating methanotrophic consumption.

4.4 Analysis of gaseous hydrocarbons heavier than methane.

C_{2+} volatile hydrocarbons (ethane, propane, butane, pentane, and hexane) in the four, high-CH_4 soil-gas samples were below the FTIR detection limit of 1 ppmv (Table S4).

4.5 Analysis of H_2 and CH_4 dissolved in spring waters

In the five springs along the Pusteria and Anterselva Valleys (Fig. 1), CH_4 concentrations were always in equilibrium with the atmosphere, and H_2 concentrations were below detection limits (1.5-2 ppmv CH_4 and 5 ppmv H_2 within the extracted head-space, respectively).

4.6 DNA and mcrA gene quantitative polymerase chain reaction –qPCR- analyses

The microbiological analyses, performed on 40 soil samples from seven drilling points, clearly indicate that CH_4-rich sites (P1 and P8) host higher amounts of methanogenic bacteria as compared to the two control (no CH_4) sites (P1-BG and P8-BG) (Table S6). As expected, the quantity of methanogens initially increased with depth following lower redox potential. However, at approximately 40-60 cm the increase was attenuated and a decrease occurred, likely due to overall harsher conditions. At one of the richest CH_4 sites (P8b), the highest concentration of active bacteria was shallower (30 cm) than for the other sites.

5. Discussion

5.1 Multiple isotopic analyses unveiled a modern microbial origin for CH_4 and CO_2

The bulk isotopic composition of CH_4 and CO_2 suggest a biological origin of these gases (Figures 3 and 4). The ^{13}C-enrichment of CH_4 at P1 ($\delta^{13}C$: -41.6 ‰) could be related to substrate depletion or oxidation (Whiticar, 1999). Although oxidation is commonly observed at shallow depths above water-logged sediments (e.g., Hornibrook et al. 1997), there is no corresponding ^{2}H-enrichment in P1 (Fig. 3). Overall, the isotopic CH_4 and CO_2 data were compatible to signatures of methyl-fermentation (Fig. 4; Whiticar, 1999). The radiocarbon content of CH_4 and CO_2 in all four CH_4-CO_2-rich sites ($F^{14}C > 1$) confirmed modern microbial origin. Accordingly, an attribution to the overlapping abiotic genetic field in the clumped isotope diagram (Fig. 3B) is excluded. Therefore, the observed CH_4 is not a geological carrier of H_2.

The radiocarbon data represent a key finding because they clarifies that H_2 is only associated with modern microbial gases, which are all typical of fermentation. Since methanogens may thrive on any type of H_2, microbial CH_4 alone does not allow us to exclude a geological origin for H_2; but the presence of microbial CO_2 corroborates an exclusion because it is typically co-produced with H_2 during acetogenesis (Ye et al. 2014).

Understanding specific CH_4 and CO_2 sources, and potential isotopic C fractionation in the soil, was beyond the scope of this study; such an undertaking requires gas and organic matter ^{14}C analyses at multiple depths (e.g. Wordell-Dietrich et al. 2020). The unequivocal isotopic data demonstrated that microbial and modern CH_4 and CO_2 can reach elevated concentrations in aerated soil (up to >50 vol.% CH_4 and >20 vol.% CO_2). Similar CH_4 and CO_2 concentrations are common in landfill soils, where waste is decomposed by aerobic methanogenesis. However, we were unable to locate any reports of such high levels of microbial gas in natural aerated soils.

Whether or not the observed large quantities of CH_4 (up to 51 vol.%) were totally or partially produced in aerated soil portions (using CO_2 and H_2 migrating from fermentation sites) remains

undetermined. Methanogenesis in the aerated soils is a known process: as in our case, it was reported around wetlands (Angle et al. 2017) and in Tyrol Alpine soils (Hofmann et al., 2016). Due to the inherent reversibility of hydrogenase-encoding enzymes, leading to either the emission or consumption of H_2, depending on fluctuating metabolic requirements (Ogata and Lubitz, 2021), the detection of specific H_2 producing bacteria remained elusive. Nevertheless, the overall bacterial population (universal for the 16S ribosomal gene), which was several orders of magnitude higher than the methanogenic population, was particularly high at the P1 site. Therefore, it is possible that such an extra population included H_2 producers. H_2-generating metabolism is widespread across very diverse prokaryotic groups, and encompasses anaerobic gram positives, enterobacteria, symbiotic or free-living nitrogen-fixing bacteria, photosynthetic cyanobacteria, and sulphur bacteria.

5.2 No evidence of crustal degassing

H_2 and tectonic faults. The Pusteria Valley develops along a regional fault system, but the spatial distribution of soil-gas H_2, derived by interpolation of the July 2021 survey data (Fig. 2), only partially coincides with two fault lineaments, the Pusteria Fault (PF) and the Kalkstein-Vallarga Fault (KV) (see Supplementary Material). The P1 H_2-rich site, located near the PF trace, actually hosts high concentrations of microbial modern CO_2, which obviously is not a result of fault degassing (Fig. 2). Rather than faults, H_2 and CO_2 appear to generally follow the valley slope and bottom, which include flat areas, channels and depressions. These are zones of low relative elevation, inducing water accumulation, shallow groundwater flows, and increased soil moisture, factors that contribute to near-surface microbial gas production (e.g., Morozumi et al. 2019). Further ^{14}C analyses should be performed in other soil-gas sites along the PF to unambiguously identify possible geological degassing processes.

No gas exhalation to the atmosphere. Dry soil is known to be a net sink of H_2, with rapid H_2 consumption corroborated by negative fluxes (Conrad, 1996; Hammer and Levin, 2009; Chen et al., 2015). The presence of advective exhalation of H_2 from the soil to the atmosphere is, therefore,

396 considered to be a potential proxy for subsurface gas migration (Etiope, 2023). The flux
397 measurements of CH_4 and H_2 obtained using the closed-chamber technique within the richest gas
398 sites during September 2021 (Fig. 1) did not show the presence of active seepage. Gas concentrations
399 within the chamber were monitored over a five-minute interval, an interval that, with the specific
400 chamber-sensor system used, is generally sufficient to detect fluxes typical of active seeps (Etiope et
401 al. 2017; Etiope, 2023). The measurements suggest that the CH_4-H_2 concentrations within the soil are
402 not due to active, pressure-driven gas migration (seepage). High gas concentrations in soil pores
403 associated with a lack of fluxes to the atmosphere are more frequently related to small, low-pressure
404 pockets of *in situ* originated gas (Forde et al. 2018; Etiope, 2023). Despite the possibility that silty
405 material and wet layers may restrict the gas flow above the soil-gas sample depth (60–80 cm), the
406 negative CH_4 flux observed in three locations, which suggests methanotrophic consumption, typical
407 of dry soil, still points to the presence of air movement in the upper soil layers.
408 *No heavier hydrocarbons in soils and no geological gas in springs*. The lack of gaseous hydrocarbons
409 heavier than methane in the soil, which may be produced in deep C-rich rocks either by thermogenesis
410 or abiotic processes (Etiope and Sherwood Lollar, 2013), and the absence of H_2 associated with CH_4
411 in atmospheric equilibrium in the several springs, are additional indicators that the investigated
412 Alpine valleys do not host an appreciable crustal degassing. Other springs in the valleys did not have
413 any features that may suggest deep geothermal or serpentinization processes (no bubbling; pH < 9;
414 https://geoportale.retecivica.bz.it/geodati.asp). There were also no manifestations of gas seepage
415 within the area (no mofettes, no vegetation stress).
416
417 *5.3. Microbiological activity in the soil*
418 Although a large methanogenic population was detected in the investigated soils, whether or not the
419 observed large quantities of CH_4 (up to 51 vol.%) were totally or partially produced in aerated soil
420 portions (using CO_2 and H_2 migrating from fermentation sites) remains undetermined.
421 Methanogenesis in the aerated soils is a known process: as in our case, it was reported around

wetlands (Angle et al. 2017) and in Tyrol Alpine soils (Hofmann et al., 2016). Due to the inherent reversibility of hydrogenase-encoding enzymes, leading to either the emission or consumption of H_2, depending on fluctuating metabolic requirements (Ogata and Lubitz, 2021), the detection of specific H_2 producing bacteria remained elusive. Nevertheless, the overall bacterial population (universal for the 16S ribosomal gene), which was several orders of magnitude higher than the methanogenic population, was particularly high at the P1 site. Therefore, it is possible that such an extra population included H_2 producers. H_2-generating metabolism is widespread across very diverse prokaryotic groups, and encompasses anaerobic gram positives, enterobacteria, symbiotic or free-living nitrogen-fixing bacteria, photosynthetic cyanobacteria, and sulphur bacteria.

5.4 Potential biogenic sources of H_2 and CO_2

Although it can be hypothesized that methanogenic activity in the meadows could have been caused by crustal H_2 degassing (where bacteria use geological H_2 as an energy source), the simultaneous presence of high quantities of microbial CO_2 and H_2S is indicative of fermentation activity. CO_2, H_2S, and H_2 are, in fact, all typical co-products of two stages of anaerobic digestion, acetogenesis (the transformation of alcohols, and carbonic and fatty acids into gases) and, subordinately, acidogenesis (the conversion of sugars and amino acids; Valdez-Vazquez and Poggi-Varaldo, 2009). H_2 is a key intermediate in anaerobic environments and these fermentation stages are particularly enhanced in wet soils (Ye et al. 2014). While it is known that methanogenesis can occur in aerated soils (Angle et al. 2017; Hoffmann et al, 2016), fermentation requires anoxic conditions. The ^{14}C content of CO_2 suggests that the C feedstock (organic matter) is approximately 1200-1400 years old at P8 ($F^{14}C_{CO2}$: 0.846) and younger, influenced by the bomb spike ($F^{14}C_{CO2}$: >1), at the other three sites. These data are typical of fermentation observed in wetlands, fens, bogs, and peat soils (Chanton et al. 2008; Trumbore et al. 1999). Although we can assume that normal soil respiration (a common process in aerobic soils, leading to CO_2 concentrations typically <1 vol.%) exists in all investigated sites, we hypothesize that the large quantities of CO_2 (up to 27 vol.%), observed at depths of 60-80 cm, are

allochthonous (as well as the associated H_2, CH_4 and H_2S), and migrated from shallow wet soil layers and/or adjacent water-logged strata (wetland, fens) that are widespread in Tyrol Alpine grasslands (Fig. 1; Hilpold et al. 2023). The A14 site is, in fact, located between two wetland zones (bogs; Fig. 1 and Fig. S1; Supplementary Material). The P8 and A15 sites are located near diffuse water-logged soils, and are likely impacted by the emergence of shallow groundwater (and by the spring in A15). High H_2 concentrations in the apparently dry meadows of P1 and other sites, such as n. 12 and 22, as observed in the September 2021 survey (Table S2), were less expected. We could not obtain specific information regarding the depth of local aquifers. However, we could not exclude the existence of substantial organic matter under anaerobic conditions at shallow depth, induced by near surface water flows (the meadows around P1 host drainage channels), as is typical of Alpine proglacial zones and hillslopes (e.g., Müller et al. 2022; Penna et al. 2015).

Delving into the particular microbiological and environmental factors that could contribute to the high amounts of H_2, CH_4, and CO_2 was beyond the purview of our study, since our goal was to exclusively figure out whether H_2 and associated gases are geological. Additional research is required to broaden the current understanding of the soil's capacity for H_2 production and syntrophic consumption (Piché-Choquette and Constant, 2019; Meinel et al. 2022). Oxygenation (H_2 was extracted from aerated soils) and H_2S (observed at the richest H_2 sites) are known to be strong inhibitors of H_2 consumption. These and other potential inhibitors, such as organic acids and alcohols (Oremland and Taylor, 1975; Hoeler et al. 1998; Schmidt et al. 2016), will be considered in future studies. Studying the variation of H_2 with depth within the soil (as suggested in Zgonnik et al., 2015) could also be considered in a future work, but in our case this approach may not be effective in determining the source of H_2: in fact, in the vadose zone H_2 may increase with depth either if the gas migrates from deeper geological formations or is generated in moist subsoil and aquifers. Geological seepage could potentially be detected exclusively through boreholes that penetrate the bedrock beneath aquifers, on the condition that artificial H_2 production associated with drilling (as documented in Halas et al. 2021) can be disregarded.

5.5 Geological or biological H_2?

Table 2 summarizes multiple indicators, considered in this work, which may suggest a geological or biological origin for the H_2 observed within the Pusteria and Anterselva Valleys. No single indicator unequivocally demonstrates that H_2 is geological. Microbial origin is, instead, supported by multiple lines of evidence. The ^{14}C-enrichment of CO_2 is, in particular, a strong indication that H_2 is also microbial. While methanogenesis near the surface may develop through the use of geological H_2, modern CO_2 is compatible with acetogenesis during fermentation, for which H_2 and H_2S (the latter was observed at high CH_4-H_2-CO_2 sites) are typical products (i.e. Ye et al. 2014). The existence of geological H_2 degassing at sites dominated by microbial gas would be a tremendous coincidence. The coexistence of crustal helium (^4He) anomalies and hydrogen in the soil was suggested as a crucial element in determining the deep source of hydrogen, hence minimizing the possibility of misinterpreting surface biological hydrogen detection (e.g., Prinzhofer et al. 2024). Nevertheless, this concept is valid only if the potential ^4He radiogenic source rocks, such as granite basement and intrusions, are quite deep (e.g., within sedimentary basins). It is well known that in areas with shallow or outcropping crystalline basement, crustal helium in soil-gas is not a deep gas tracer, but it reflects groundwater circulation in fractured igneous rocks at shallow depths (e.g., Gregory and Durrance, 1987; Gascoyne et al. 1993). Therefore, detecting ^4He soil-gas anomalies in the Pusteria region, where the Australpine crystalline basement is exposed (Supplementary Material), may not be conclusive. Mantle-derived ^3He is virtually absent in near-surface groundwaters of the Central and Eastern Alps (Marty et al. 1992).

6. Conclusions

The results of this work suggest that aerated soils may host considerable amounts of microbial H_2, as observed for CH_4. This phenomenon should be considered in surface H_2 exploration guidelines. Caution should, then, be paid when interpreting concentrations of H_2 in the soil in the order of 10^2-10^3 ppmv, as in the case of the so-called "fairy circles" or "sub-circular depressions", which may host wet ground. Cursorily attributing a geological origin to H_2 in the soil, without a rigorous analysis of the isotopic composition of the associated gases, can be misleading. We demonstrated that radiocarbon analysis of CH_4 and CO_2 is a decisive interpretative tool.

The detected concentrations of microbial CH_4 and CO_2 also appear to be the highest ever reported in the scientific literature for aerated soils. In this respect, our study represents a new reference for the potential of microbial C-bearing gas production and greenhouse-gas cycle in surface environments. Future research should address the biological reasons for the high H_2 levels, and related modern CO_2 and CH_4, focusing on the potential H_2 consumption inhibitors, such as oxygen, sulphide, organic acids and alcohols. Acquiring further soil-gas and flux data in aerated and wet soils will be beneficial not only for improving natural CH_4 emission estimates, but also for expanding the dataset of surface biological H_2 generation, an essential baseline for the ongoing geological and geochemical exploration of natural hydrogen.

Data availability.

All data acquired in this study are available in this paper and Supplementary data file.

Declaration of competing interests

The authors declare no competing interests or personal relationships that could have appeared to influence the work reported in this paper.

Acknowledgements

We acknowledge support from the Istituto Nazionale di Geofisica e Vulcanologia ("Sezione Roma 2 - Etiope" project funds) and the Project SID (Investimento Strategico di Dipartimento) 2021 of University of Padova. M. Sivan and the Thermo Ultra instrument are supported by the Netherlands Earth Science System Center (NESSC), funded by the Ministry of Education, Culture and Science (OCW) and Utrecht University. We thank C. van der Veen for the isotopic analyses at Utrecht University. R. Conrad, C. Vogt, and M.E. Popa offered

fruitful discussions on biological H_2 production. A. Tondello is gratefully acknowledged for assistance in the DNA amplification analyses and P. Stevanato for the availability of required facilities. We also thank L. Ruggiero for help with soil sampling.

Author contributions. GE designed the multidisciplinary study, executed field measurements and laboratory FTIR analyses, interpreted all data, and developed the manuscript. GC, EB, RS and CM executed field measurements, contributed to geological analysis and mapping. TR and MS performed methane bulk and clumped isotope analyses. AS performed the microbiological analyses. TL, SS and NH performed the ^{14}C analyses. All authors contributed to data interpretation and manuscript refinement.

Supplementary Material

Supplementary text, figures and tables are annexed to this paper.

References

Angle, J.C., Morin, T.H., Solden, L.M., Narrowe, A.B., Smith, G.J., Borton, M.A., et al. (2017). Methanogenesis in oxygenated soils is a substantial fraction of wetland methane emissions. Nature Comm., 8, 1567, doi.org/10.1038/s41467-017-01753-4.

Benà, E., Ciotoli, G., Ruggiero, L., Coletti, C., Bossew, P., Massironi, M., et al. (2022). Evaluation of tectonically enhanced radon in fault zones by quantification of the radon activity index. Scientific Reports, 12, 21586.

Boreham, C.J., Edwards, D.S., Czado, K., Rollet, N.,Wang, L., van der Wielen, S., et al. (2021). Hydrogen in Australian natural gas: occurrences, sources and resources. The APPEA J., 61, 63-91.

Brass, M., Röckmann, T. (2010). Continuous-flow isotope ratio mass spectrometry method for carbon and hydrogen isotope measurements on atmospheric methane, Atmos. Meas. Tech., 3, 1707-1721.

Carrillo Ramirez, A., Gonzalez Penagos, F., Rodriguez, G., Moretti, I. (2023). Natural H_2 emissions in Colombian ophiolites: first findings. Geosciences, 13, 358.

Chanton, J.P., Glaser, P.H., Chasar, L.S., Burdige, D.J., Hines, M.E., Siegel, D.I., Tremblay, L.B., Cooper, W.T. (2008). Radiocarbon evidence for the importance of surface vegetation on fermentation

564 and methanogenesis in contrasting types of boreal peatlands. Global Biogeoch. Cycles 22, GB4022,
565 doi:10.1029/2008GB003274.
566
567 Chen Q., Popa M.E., Batenburg A.M., Röckmann T. (2015). Isotopic signatures of production and
568 uptake of H_2 by soil. Atmos. Chem. Phys., 15, 13003-21.
569
570 Conrad, R. (1996). Soil microorganisms as controllers of atmospheric trace gases (H_2, CO, CH_4, OCS,
571 N_2O, and NO). Microbiol. Rev., 60, 609-640.
572
573 Conrad, R., Seiler, W. (1980) Contribution of hydrogen production by biological nitrogen fixation to
574 the global hydrogen budget. J. Geoph. Res., Oceans, 85(C10), 5493-5498.
575
576 Dunham, E.C., Dore, J.E., Skidmore, M.L. (2021). Lithogenic hydrogen supports microbial primary
577 production in subglacial and proglacial environments. PNAS, 118, e2007051117.
578
579 Espic, C., Liechti, M., Battaglia, M., Paul, D., Röckmann, T., Szidat, S. (2019). Compound-specific
580 radiocarbon analysis of atmospheric methane: a new preconcentration and purification setup.
581 Radiocarbon, 61, 1461-1476, doi.org/10.1017/RDC.2019.76.
582
583 Etiope, G. (2023). Massive release of natural hydrogen from a geological seep (Chimaera, Turkey):
584 gas advection as a proxy of subsurface gas migration and pressurised accumulations. Int. J. Hydrogen
585 Energy, 48, 9172-9184, doi.org/10.1016/j.ijhydene.2022.12.025.
586
587 Etiope, G., Doezema, L., Pacheco, C. (2017). Emission of methane and heavier alkanes from the La
588 Brea Tar Pits seepage area, Los Angeles. J. Geophys. Res. Atm., 122, 12,008-12,019. doi:
589 10.1002/2017JD027675.
590
591 Etiope, G., Oze, C. (2022). Microbial vs abiotic origin of methane in continental serpentinized
592 ultramafic rocks: a critical review and the need of a holistic approach. App. Geochem., 143, 105373,
593 doi.org/10.1016/j.apgeochem.2022.105373
594
595 Etiope, G., Sherwood Lollar, B. (2013). Abiotic methane on Earth. Rev. Geophys. 51, 276–299,
596 doi.org/10.1002/rog.20011.
597

598 Forde, O.N., Mayer, K.U., Cahill, A.G., Mayer, B., Cherry, J.A., Parker, B.L. (2018). Vadose zone
599 gas migration and surface effluxes after a controlled natural gas release into an unconfined shallow
600 aquifer. Vadose Zone, 17, 180033.
601
602 Frery, E., Langhi, L., Maison, M., Moretti, I. (2021). Natural hydrogen seeps identified in the north
603 Perth Basin, western Australia. Int. J. Hydrogen Energy, 46, 31158-73.
604
605 Gascoyne, M., Wuschke, D.M., Durrance, E.M. (1993). Fracture detection and groundwater flow
606 characterization using He and Rn in soil gases, Manitoba, Canada. Appl. Geochem., 8, 223-233.
607
608 Gaucher, E.C. (2020). New perspectives in the industrial exploration for native hydrogen. Elements
609 16, 8-9.
610
611 Geymond, U., Briolet, T., Combaudon, V., Sissmann, O., Martinez, I., Duttine, M., Moretti, I. (2023).
612 Reassessing the role of magnetite during natural hydrogen generation. Frontiers in Earth Science, 11,
613 1169356.
614
615 Gregory, R.G., Durrance, E.M. (1987). Helium in soil gas: a method of mapping groundwater
616 circulation systems in fractured plutonic rock. Appl. Geochem., 2, 11-23.
617
618 Halas, P., Dupuy, A., Franceschi, M., Bordmann, V., Fleury, J.M., Duclerc, D. (2021). Hydrogen
619 gas in circular depressions in South Gironde, France: Flux, stock, or artefact? App. Geochem., 127,
620 104928.
621
622 Hammer, S., Levin, I. (2009). Seasonal variation of the molecular hydrogen uptake by soils inferred
623 from continuous atmospheric observations in Heidelberg, southwest Germany. Tellus B: Chemical
624 and Physical Meteorology, 61, doi:10.1111/j.1600-0889.2009.00417.x.
625
626 Hilpold, A., Anderle, M., Guariento, E., Marsoner, T., Mina, M., Paniccia, C., Plunger, J., Rigo, F.,
627 Rüdisser J., Scotti, A., Seeber, J., Steinwandter, M., Stifter, S., Strobl, J., Suarez-Muñoz, M., Vanek,
628 M., Bottarin, R., Tappeiner, U. (2023). Biodiversity Monitoring South Tyrol - Handbook,
629 Bozen/Bolzano, Italy, Eurac Research, doi.org/10.57749/2qm9-fq40
630

631 Hinkle, M. (1994). Environmental conditions affecting concentrations of He, CO_2, O_2 and N_2 in soil
632 gases. Appl. Geochem. 9, 53–63.
633
634 Hoehler, T.M., Alperin, M.J., Albert, D.B., Martens, C.S. (1998). Thermodynamic control on
635 hydrogen concentrations in anoxic sediments. Geochim. Cosmoch. Acta, 62, 1745-1756.
636
637 Hofmann, K., Praeg, N., Mutschlechner, M., Wagner, A.O., Illmer, P. (2016). Abundance and
638 potential metabolic activity of methanogens in well-aerated forest and grassland soils of an alpine
639 region. FEMS microbiology ecology, 92(2), fiv171.
640
641 Hornibrook, E.R., Longstaffe, F.J., Fyfe, W.S. (1997). Spatial distribution of microbial methane
642 production pathways in temperate zone wetland soils: Stable carbon and hydrogen isotope evidence.
643 Geochim. Cosmoch. Acta, 61, 745-753.
644
645 IEA (2023). Global Hydrogen Review 2023, IEA, Paris https://www.iea.org/reports/global-
646 hydrogen-review-2023,
647
648 Kinnaman, F.S., Valentine, D.L., Tyler, S.C. (2007). Carbon and hydrogen isotope fractionation
649 associated with the aerobic microbial oxidation of methane, ethane, propane and butane. Geochim.
650 Cosmochim. Acta 71, 271–283.
651
652 Krämer, H., Conrad, R. (1993). Measurement of dissolved H_2 concentrations in methanogenic
653 environments with a gas diffusion probe. FEMS Microbiology Ecology, 12, 149-158.
654
655 Langhi, L., Strand, J. (2023). Exploring natural hydrogen hotspots: a review and soil-gas survey
656 design for identifying seepage. Geoenergy, 1, doi.org/10.1144/geoenergy2023-014.
657
658 Larin, N., Zgonnik, V., Rodina, S., Deville, E., Prinzhofer, A., Larin, V.N. (2015). Natural molecular
659 hydrogen seepage associated with surficial, rounded depressions on the European craton in Russia.
660 Nat. Resour. Res., 24, 369-383.
661
662 Lefeuvre, N., Truche, L., Donz., F.-V., Ducoux, M., Barr., G., Fakoury, R.-A., et al. (2021). Native
663 H_2 exploration in the western Pyrenean foothills. Geochemistry, Geophysics, Geosystems, 22,
664 e2021GC009917, doi.org/10.1029/2021GC009917

Lévy, D., Roche, V., Pasquet, G., Combaudon, V., Geymond, U., Loiseau, K., Moretti, I. (2023). Natural H_2 exploration: tools and workflows to characterize a play. Sci. Tech. Energ. Transition, 78, 27, doi.org/10.2516/stet/2023021

Marty, B., O'Nions, R.K., Oxburgh, E.R., Martel, D., Lombardi, S. (1992). Helium isotopes in Alpine regions. Tectonophysics, 206, 71-78.

Mathur, Y., Awosiji, V., Mukerji, T., Scheirer, A.H., Peters, K.E. (2023). Soil geochemistry of hydrogen and other gases along the San Andreas fault. Int. J. Hydrogen Energy, 50, 411-419.

McMahon, C.J., Roberts, J.J., Johnson, G., Edlmann, K., Flude, S., Shipton, Z.K. (2023). Natural hydrogen seeps as analogues to inform monitoring of engineered geological hydrogen storage. Geol Soc Spec Publ., 528, doi.org/10.1144/SP528-2022-5.

Meinel, M., Delgado, A.G., Ilhan, Z.E., Aguero, M.L., Aguiar, S., Krajmalnik-Brown, R., Torres, C.I. (2022). Organic carbon metabolism is a main determinant of hydrogen demand and dynamics in anaerobic soils. Chemosphere, 303, 134877.

Milkov, A.V. (2022). Molecular hydrogen in surface and subsurface natural gases: abundance, origins and ideas for deliberate exploration. Earth Sci. Rev., 104063.

Milkov, A.V., Etiope, G. (2018). Revised genetic diagrams for natural gases based on a global dataset of >20,000 samples. Org. Geochem. 125, 109–120.

Moretti, I., Geymond, U., Pasquet, G., Aimar, L., Rabaute, A. (2022). Natural hydrogen emanations in Namibia: field acquisition and vegetation indexes from multispectral satellite image analysis. Int. J. Hydrogen Energy, 47, 35588-607.

Morozumi, T., Shingubara, R., Suzuki, R., Kobayashi, H., Tei, S., Takano, S., et al. (2019). Estimating methane emissions using vegetation mapping in the taiga–tundra boundary of a north-eastern Siberian lowland. Tellus B: Chem. Phys. Meteor., 71(1), 1581004.

Müller, T., Lane, S.N., Schaefli, B. (2022). Towards a hydrogeomorphological understanding of proglacial catchments: an assessment of groundwater storage and release in an Alpine catchment. Hydrology and Earth System Sciences, 26(23), 6029-6054.

Newell, K.D., Doveton, J.H., Merriam, D.F., Gilevska, T., Waggoner, W.M., Magnuson, L.M. (2007). H_2-rich and hydrocarbon gas recovered in a deep Precambrian well in Northeastern Kansas. Nat. Resour. Res., 16, 277–292.

Ogata, H., Lubitz, W. (2021). Bioenergetics Theory and Components | Hydrogenases Structure and Function, Editor: J. Jez, Encyclopedia of Biological Chemistry III (Third Edition), Elsevier, 66-73.

Oremland, R.S., Taylor, B.F. (1975). Inhibition of methanogenesis in marine sediments by acetylene and ethylene: validity of the acetylene reduction assay for anaerobic microcosms. App. Microbiol., 30, 707-709.

Osselin, F., Soulaine, C., Fauguerolles, C., Gaucher, E. C., Scaillet, B., Pichavant, M. (2022). Orange hydrogen is the new green. Nature Geoscience, 15, 765-769.

Pal, D.S., Tripathee, R., Reid, M.C., Schäfer, K.V., Jaffé, P.R. (2018). Simultaneous measurements of dissolved CH_4 and H_2 in wetland soils. Environm. Monitor. Assess., 190, 1-11.

Pathirana, S.L., van der Veen, C., Popa, M.E., Röckmann, T. (2015). An analytical system for stable isotope analysis on carbon monoxide using continuous-flow isotope-ratio mass spectrometry, Atmos. Meas. Tech., 8, 5315-5324, 10.5194/amt-8-5315-2015.

Paulot, F., Paynter, D., Naik, V., Malyshev, S., Menzel, R., Horowitz, L.W. (2021). Global modeling of hydrogen using GFDL-AM4.1: Sensitivity of soil removal and radiative forcing. Int. J. Hydrogen Energy, 46, 13446-13460.

Penna, D., Mantese, N., Hopp, L., Dalla Fontana, G., Borga, M. (2015). Spatio-temporal variability of piezometric response on two steep alpine hillslopes. Hydrological Processes, 29, 198-211.

Piché-Choquette, S., Constant, P. (2019). Molecular hydrogen, a neglected key driver of soil biogeochemical processes. Appl. Environm. Microbiology, 85, e02418-18.

Prinzhofer, A., Cissé, C.S.T., Diallo, A.B. (2018). Discovery of a large accumulation of natural hydrogen in Bourakebougou (Mali). Int. J. Hydrogen Energy, 43, 19315–19326.

Prinzhofer, A., Moretti, I., Francolin, J., Pacheco, C., d'Agostino, A., Werly, J., et al. (2019). Natural hydrogen continuous emission from sedimentary basins: the example of a Brazilian H2-emitting structure. Int. J. Hydrogen Energy, 44, 5676-85.

Prinzhofer, A., Rigollet, C., Lefeuvre, N., Françolin, J., de Miranda, P.E.V. (2024). Maricá (Brazil), the new natural hydrogen play which changes the paradigm of hydrogen exploration. Int. J. Hydrogen Energy, 62, 91-98.

Rhee, T.S., Brenninkmeijer, C.A.M., Röckmann, T. (2006). The overwhelming role of soils in the global atmospheric hydrogen cycle. Atmos. Chem. Phys., 6, 1611–1625, doi.org/10.5194/acp-6-1611-2006.

Rigollet, C., Prinzhofer, A. (2022). Natural Hydrogen: a new source of carbon-free and renewable energy that can compete with hydrocarbons. First Break, 40, 78-84.

Röckmann, T., Eyer, S., van der Veen, C., Popa, M. E., Tuzson, B., et al. (2016). In situ observations of the isotopic composition of methane at the Cabauw tall tower site, Atmos. Chem. Phys., 16, 10469-10487, doi.org/10.5194/acp-16-10469-2016.

Ruff, M., Wacker, L., Gäggeler, H.W., Suter, M., Synal, H.-A., Szidat, S. (2007). A gas ion source for radiocarbon measurements at 200 kV. Radiocarbon, 49, 307-314, doi.org/10.1017/S0033822200042235.

Schmidt, O., Hink, L., Horn, M.A., Drake, H.L. (2016). Peat: home to novel syntrophic species that feed acetate- and hydrogen-scavenging methanogens. The ISME journal, 10, 1954-1966.

Sherwood Lollar, B., Onstott, T.C., Lacrampe-Couloume, G., Ballentine, C.J. (2014). The contribution of the Precambrian continental lithosphere to global H_2 production. Nature 516, 379–382. doi:10.1038/nature14017

766 Sivan, M., Röckmann, T., van der Veen, C., Popa, M.E. (2023). Extraction, purification, and clumped
767 isotope analysis of methane ($\Delta^{13}CDH_3$ and $\Delta^{12}CD_2H_2$) from sources and the atmosphere, EGUsphere,
768 1-35, 10.5194/egusphere-2023-1906.
769
770 Starkey, R.L., Wight, K.M. (1945). Anaerobic corrosion of iron in soil. American Gas Association,
771 New York, pp.108.
772
773 Sugimoto, A., Fujita, N. (2006). Hydrogen concentration and stable isotopic composition of methane
774 in bubble gas observed in a natural wetland. Biogeochemistry, 81, 33-44.
775
776 Sugisaki, R., Ido, M., Takeda, H., Isobe, Y., Hayashi, Y., Nakamura, N., et al. (1983). Origin of
777 hydrogen and carbon dioxide in fault gases and its relation to fault activity. J. Geol. 91, 239–258.
778
779 Trumbore, S.E., Bubier, J.L., Harden, J.W., Crill, P.M. (1999). Carbon cycling in boreal wetlands: a
780 comparison of three approaches. J. Geophys. Res., Atmospheres 104, D22, 27673-27682.
781
782 Umezawa, T., Brenninkmeijer, C. A. M., Röckmann, T., van der Veen, C., Tyler, S. C., Fujita, R.,
783 Morimoto, S., Aoki, S., Sowers, T., Schmitt, J., Bock, M., Beck, J., Fischer, H., Michel, S. E.,
784 Vaughn, B. H., Miller, J. B., White, J. W. C., Brailsford, G., Schaefer, H., Sperlich, P., Brand, W. A.,
785 Rothe, M., Blunier, T., Lowry, D., Fisher, R. E., Nisbet, E. G., Rice, A. L., Bergamaschi, P., Veidt,
786 C., Levin, I. (2018). Interlaboratory comparison of $\delta^{13}C$ and δD measurements of atmospheric CH_4
787 for combined use of data sets from different laboratories. Atmos. Meas. Tech. 11(2), 1207-1231,
788 doi.org/10.5194/amt-11-1207-2018.
789
790 Vacquand, C., Deville, E., Beaumont, V., Guyot, F., Sissmann, O., Pillot, D., Arcilla, C., Prinzhofer,
791 A. (2018). Reduced gas seepages in ophiolitic complexes: evidences for multiple origins of the H_2-
792 CH_4-N_2 gas mixtures. Geochem. Cosmochim. Acta 233, 437–461.
793
794 Valdez-Vazquez, I., Poggi-Varaldo, H.M. (2009). Hydrogen production by fermentative consortia.
795 Renewable and sustainable energy reviews, 13, 1000-1013.
796
797
798 Warr, O., Giunta, T., Ballentine, C.J., Sherwood Lollar, B. (2019). Mechanisms and rates of ^4He,
799 ^{40}Ar, and H_2 production and accumulation in fracture fluids in Precambrian Shield environments.

Chem. Geol. 530, 119322, doi:10.1016/j.chemgeo.2019.119322

Whiticar, M.J. (1999). Carbon and hydrogen isotope systematics of bacterial formation and oxidation of methane. Chemical Geology, 161, 291-314.

Wordell-Dietrich, P., Wotte, A., Rethemeyer, J., Bachmann, J., Helfrich, M., Kirfel, K., Leuschner, C., Don, A. (2020). Vertical partitioning of CO_2 production in a forest soil. Biogeosciences, 17, 6341–6356, doi.org/10.5194/bg-17-6341-2020.

Xiang, Y., Sun, X., Liu, D., Yan, L., Wang, B., Gao, X. (2020). Spatial distribution of Rn, CO_2, Hg, and H_2 concentrations in soil gas across a thrust fault in Xinjiang, China. Front. Earth Sci., 8, doi.org/10.3389/feart.2020.554924.

Ye, R., Jin, Q., Bohannan, B., Keller, J.K., Bridgham, S.D. (2014). Homoacetogenesis: a potentially underappreciated carbon pathway in peatlands. Soil Biology and Biochemistry, 68, 385-391.

Yedinak, E.M. (2022). The curious case of geologic hydrogen: assessing its potential as a near-term clean energy source. Joule, 6, 503-508.

Young, E.D., Kohl, I.E., Sherwood Lollar, B., Etiope, G., Rumble III, D., Li, S., Haghnegahdar, M. A., Schauble, E.A., McCain, K.A., Foustoukos, D.I., Sutclife, C., Warr, O., Ballentine, C.J., Onstott, T.C., Hosgormez, H., Neubeck, A., Marques, J.M., Pérez-Rodríguez, I., Rowe, A.R., LaRowe, D.E., Magnabosco, C., Yeung, L.Y, Ash, J.L., Bryndzia, L.T. (2017). The relative abundances of resolved $^{12}CH_2D_2$ and $^{13}CH_3D$ and mechanisms controlling isotopic bond ordering in abiotic and biotic methane gases. Geochim. Cosmochim. Acta 203, 235-264, doi.org/10.1016/j.gca.2016.12.041.

Zgonnik, V. (2020). The occurrence and geoscience of natural hydrogen: a comprehensive review. Earth Sci Rev., 203, 103140.

Zgonnik, V., Beaumont V., Deville E., Larin N., Pillot D., Farrell K.M. (2015). Evidence for natural molecular hydrogen seepage associated with Carolina bays (surficial, ovoid depressions on the Atlantic Coastal Plain, Province of the USA). Prog Earth Planet Sci., 2, 31.

Figure captions

Figure 1. Location map of soil-gas surveys and the richest H_2-CH_4-CO_2 sites within the Pusteria and Anterselva Valleys. All data are provided in Table S2. Springs where dissolved gas was examined: S- Salomone; C- Casanova Neuhaus; T- Teodone fountain; TM- Teodone Museum; G- San Giovanni. Faults: DAV- Deffereggen-Anterselva-Valles Fault (mylonitic zone); KV- Kalkstein-Vallarga Fault; PF- Pusteria Fault. Geology and faults are from Benà et al. (2022). Geological details are provided in the Supplementary Material. Wetland location was extracted from the WebGIS of the Bolzano Province (Geoportale Alto Adige, https://geoportale.retecivica.bz.it/geodati.asp).

Figure 2. **The spatial distribution of H_2 and CO_2 in soil-gas along the Pusteria Valley.** Contour lines were derived by Natural Neighbour interpolation of July 2021 soil-gas sampling points (black dots). Green stars refer to the H_2-CH_4-CO_2 rich sites, also observed in all successive soil-gas surveys. Diamonds indicate other sites with high H_2 and CH_4 concentration (up to 370 ppmv and 9000 ppmv, respectively) observed during September 2021. Map base is from Digital Elevation Model (DEM) with resolution of 2.5 m. Wetland zones (brown squares) and faults are as shown in Fig. 1.

Figure 3. The bulk (A) and clumped (B) CH_4 isotopic composition in H_2-enriched soil-gas samples of the Pusteria (P1, P8) and Anterselva (A14, A15) Valleys. Data from IMAU Lab (Table 1). CR: Carbonate Reduction; F: Fermentation. Genetic plots: A, after Milkov and Etiope, (2018); B, after Etiope and Oze, (2022). Microbial oxidation trend (red dashed arrow in A) based on the $\delta^{13}C_{CH4}$–$\delta^{2}H_{CH4}$ correlated variations with $\Delta H/\Delta C \sim 8–9$ (Kinnaman et al., 2007). ^{13}C-enrichment of P1 may reflect ^{13}C-enriched CO_2 (Table 1) and substrate depletion. Paired with the modern ^{14}C dating (Table 1), the bulk and clumped-isotopes signatures (within overlapping microbial-abiotic genetic zonation) are all attributable to microbial origin. Measurement uncertainties do not extend beyond symbol size.

Figure 4. The four H_2-rich samples, P1, P8, A14 and A15, within the combination of $\delta^{13}C_{CH4}$ and $\delta^{13}C_{CO2}$ for microbial gas. The carbon isotope partitioning trajectories resulting from both methanogenesis and oxidation processes are shown (redrawn from Whiticar, 1999). Isotopic data are from the LARA-ETH analyses of CO_2 and CH_4 executed in the same gas samples (Table S3).

Table captions

Table 1. Mean values of the isotopic composition of CH_4 (bulk, clumped, radiocarbon) and CO_2 (stable carbon and radiocarbon) at the four, H_2-rich soil-gas sampling sites. The complete dataset is reported in Table S3. Gas samples were collected at the same sampling points at different times (within 30 min) and analysed in two different laboratories (see Methods).

Table 2. A synopsis of indicators supporting a biological or geological origin for H_2 within the studied Alpine Valleys.

Table 1. Mean values of the isotopic composition of CH_4 (bulk, clumped, radiocarbon) and CO_2 (stable carbon and radiocarbon) at the four, H_2-rich soil-gas sampling sites. The complete dataset is reported in Table S3. Gas samples were collected at the same sampling points at different times (within 30 min) and analysed in two different laboratories (see Methods).

site	*IMAU Lab*				LARA – ETH Lab			
	$\delta^{13}C_{CH4}$ ‰	$\delta^{2}H_{CH4}$ ‰	$\Delta^{13}CH_3D$ ‰	$\Delta^{12}CH_2D_2$ ‰	$\delta^{13}C_{CH4}$ ‰	$F^{14}C_{CH4}$	$\delta^{13}C_{CO2}$ ‰	$F^{14}C_{CO2}$
P1	-41.6	-348.2	-0.21	-29.4	-42.4	1.045	-17.9	1.022
P8	-64.4	-321.8	nm	nm	-65.3	1.048	-21.2	0.846
A14	-68.6	-289.1	nm	nm	-67.0	1.163	-20.7	1.095
A15	-62.7	-318.3	1.78	-23.1	-63.5	1.019	-23.4	1.025

nm: not measured. The uncertainties are indicated in Methods and Supplementary Information. Stable C and H isotopic ratios are relative to VPDB (Vienna Pee-Dee-Belemnite) and VSMOW (Vienna Standard Mean Ocean Water), respectively.

Table 2. A synopsis of indicators supporting a biological or geological origin for H_2 within the studied Alpine Valleys.

		Geo H_2	Bio H_2	Notes
1	High soil-gas H_2 concentrations	X	?	Limited literature data on bio-H_2 in soils
2	H_2 near wetland or water-logged soil		X	
3	H_2 coupled to microbial-modern CH_4	X	X	Surface methanogenesis could be developed using geological H_2
4	Presence of methanogens in the soil	X	X	
5	H_2 coupled to biological (^{13}C-depleted) CO_2		X	
6	H_2 coupled to modern (^{14}C-enriched) CO_2		X	
7	No positive H_2 flux from the soil		X	Wet soil layers may inhibit gas exhalation
8	No H_2 or CH_4 in spring water		X	
9	No clear spatial relationship between H_2 and faults		X	
10	Lack of geothermal or serpentinization fluids in springs		X	

Figure 1

Click here to access/download;Figure;Stoten Fig1.tiff

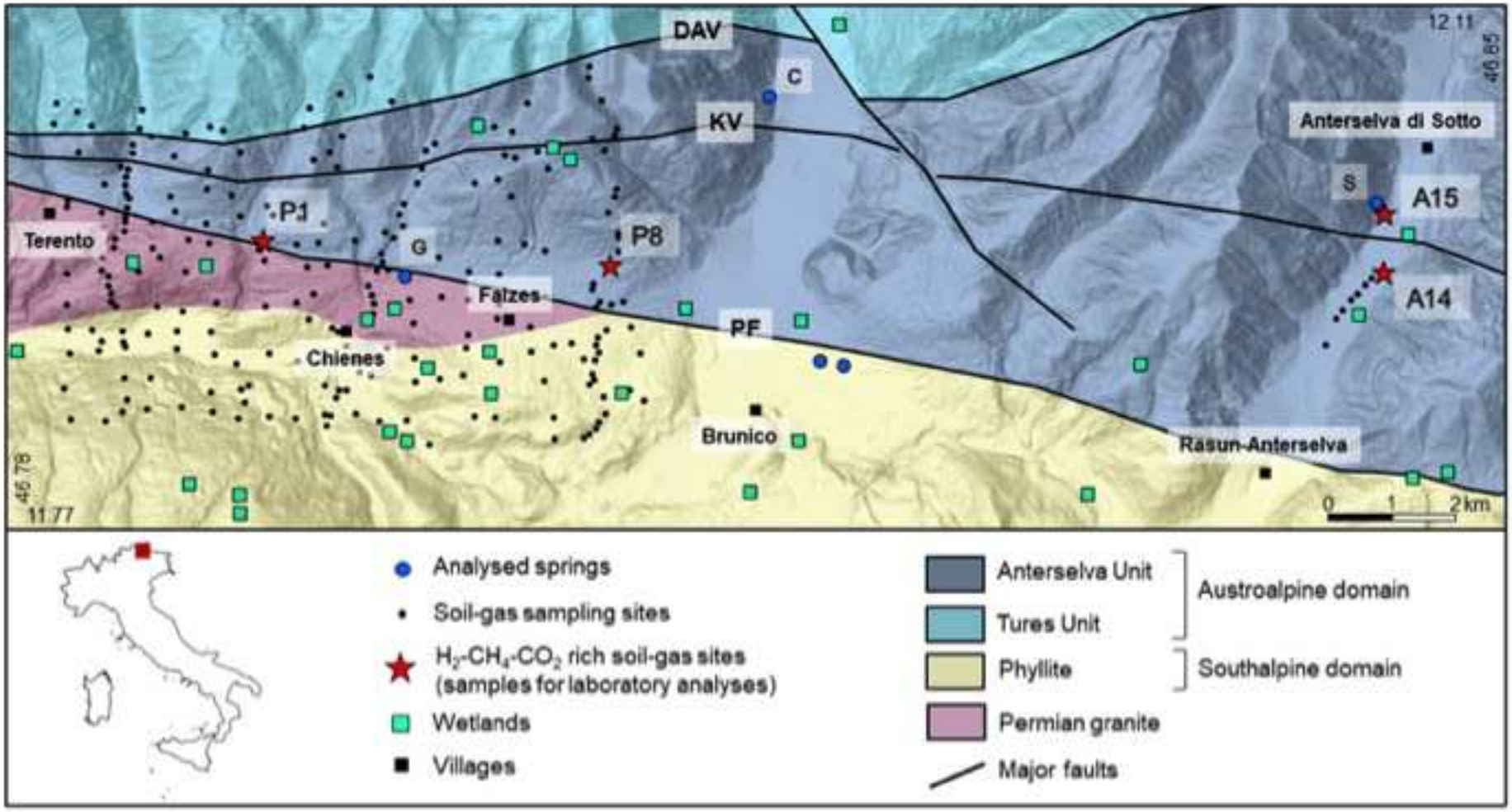

Figure 2

Click here to access/download;Figure;Stoten Fig2 new.tiff

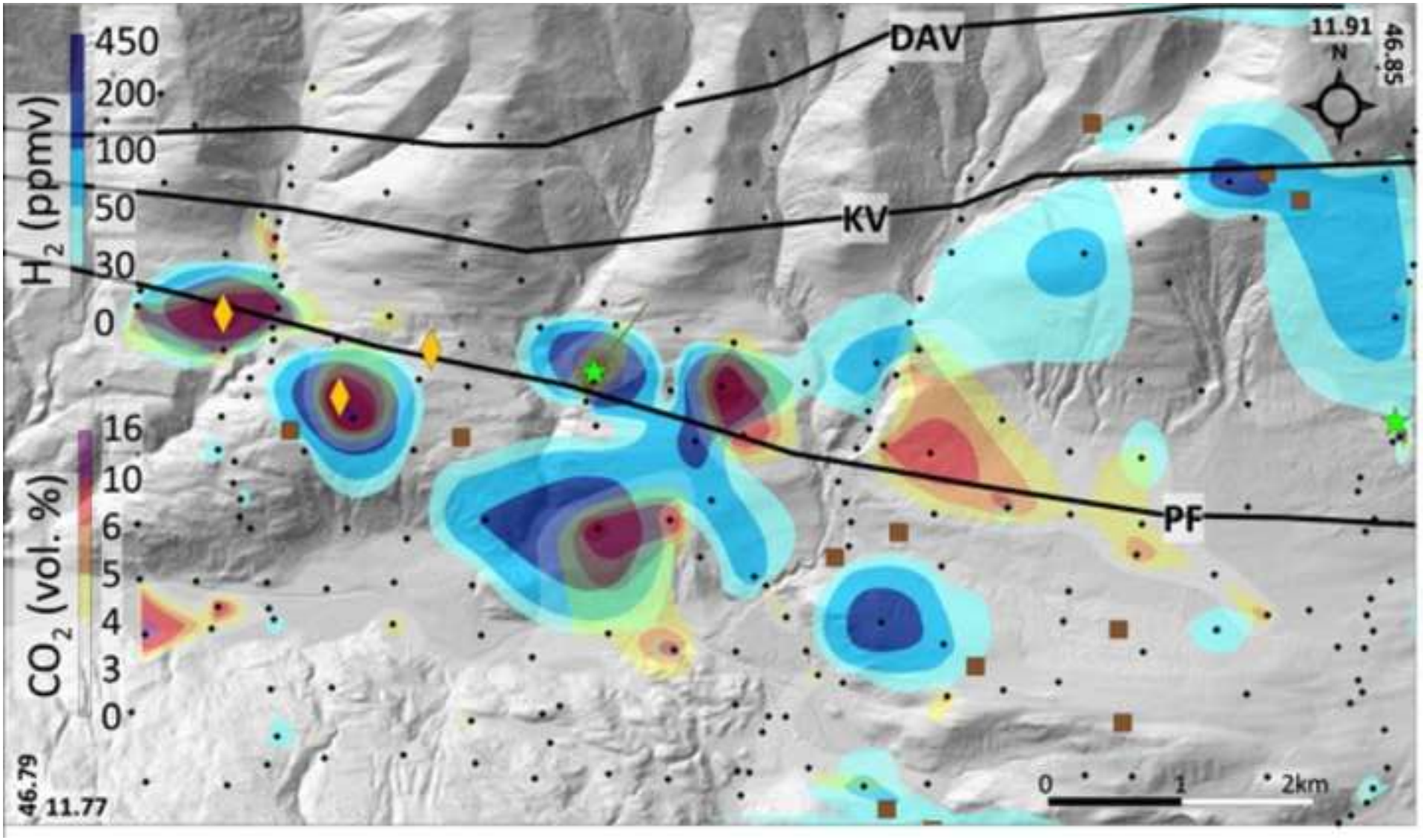

Figure 3

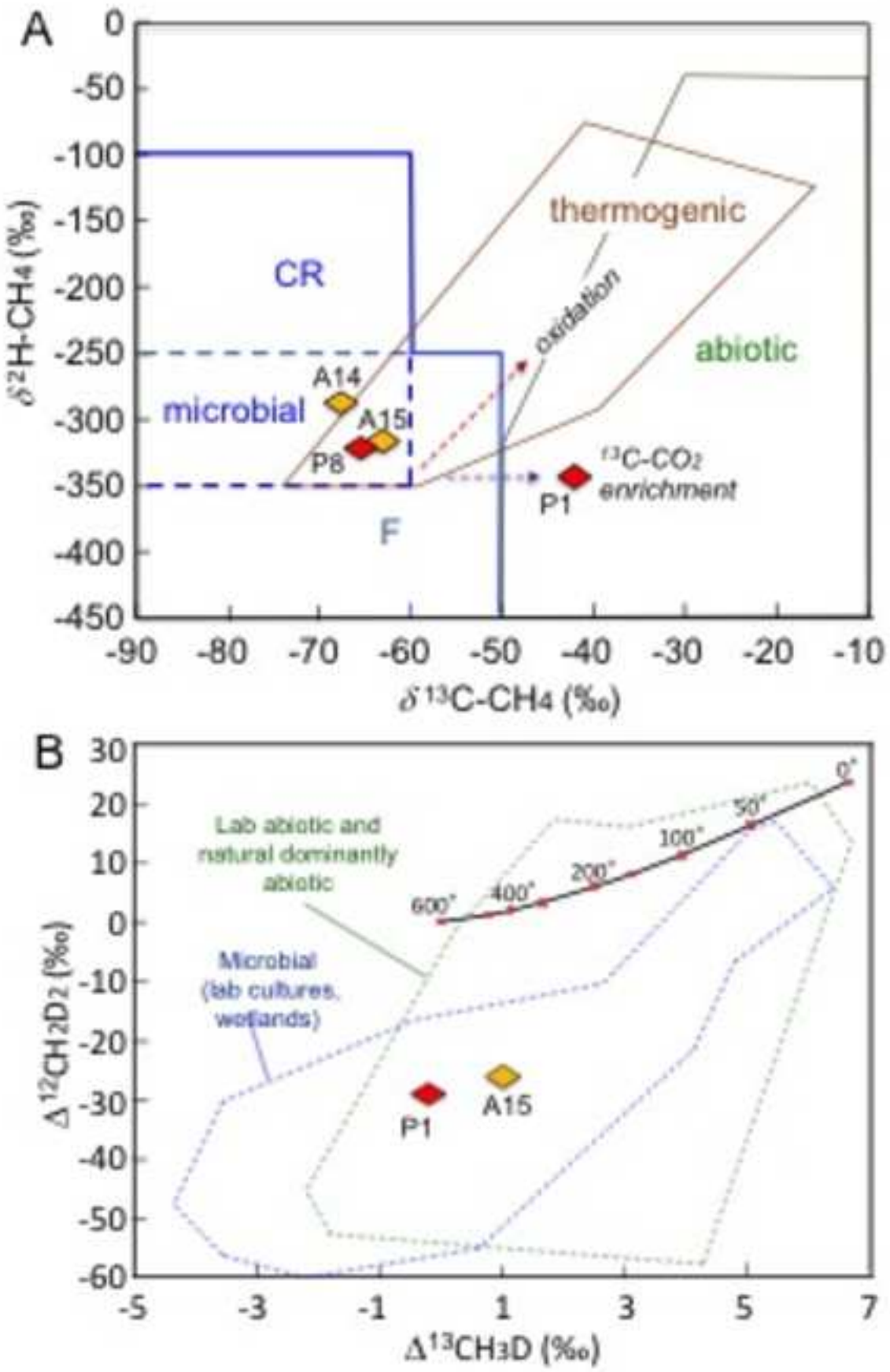

Figure 4

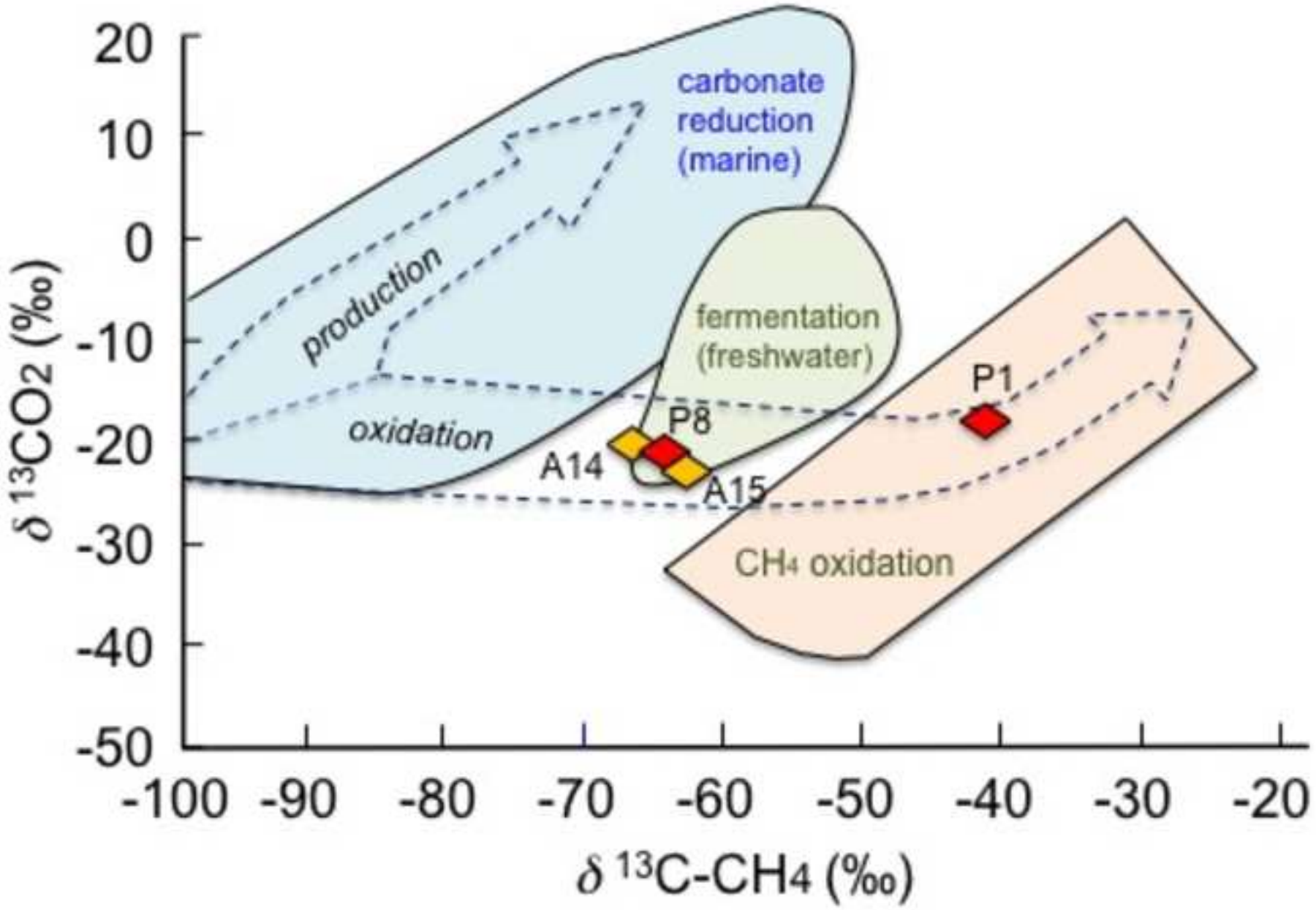

Declaration of competing interests

The authors declare no competing interests or personal relationships that could have appeared to influence the work reported in this paper.